Biochemical Pharmacology 216 (2023) 115770

Contents lists available at ScienceDirect

Biochemical Pharmacology

journal homepage: www.elsevier.com/locate/biochempharm

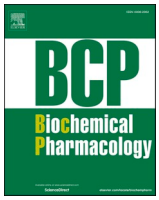

Review

High throughput microscopy and single cell phenotypic image-based analysis in toxicology and drug discovery

Fabio Stossi [a,b,*], Pankaj K. Singh [b,c], Kazem Safari [b,c], Michela Marini [b,d], Demetrio Labate [b,d], Michael A. Mancini [a,b,c,*]

[a] Department of Molecular and Cellular Biology, Baylor College of Medicine, Houston, TX, USA
[b] GCC Center for Advanced Microscopy and Image Informatics, Houston, TX, USA
[c] Center for Translational Cancer Research, Institute of Biosciences and Technology, Texas A&M University, Houston, TX, USA
[d] Department of Mathematics, University of Houston, Houston, TX, USA

ARTICLE INFO

Keywords:
High throughput microscopy
Phenotypic heterogeneity
Artificial intelligence
Image analysis

ABSTRACT

Measuring single cell responses to the universe of chemicals (drugs, natural products, environmental toxicants etc.) is of paramount importance to human health as phenotypic variability in sensing stimuli is a hallmark of biology that is considered during high throughput screening. One of the ways to approach this problem is via high throughput, microscopy-based assays coupled with multi-dimensional single cell analysis methods. Here, we will summarize some of the efforts in this vast and growing field, focusing on phenotypic screens (*e.g.,* Cell Painting), single cell analytics and quality control, with particular attention to environmental toxicology and drug screening. We will discuss advantages and limitations of high throughput assays with various end points and levels of complexity.

1. Introduction

The traditional and mostly successful scheme for high throughput screening (HTS) of compounds, drugs, and environmental toxicants has been to test large number of chemical moieties against disease-relevant, specific molecular targets, largely employing synthetic systems (*i.e.,* purified targets, binding assays, engineered reporters etc.) without considering the cellular milieu and the complexity of the variation of responses at the single cell level. The molecular pathways in a cell form an intricate web of possible outputs to each natural or synthetic stimulus, integrated with positive and negative feedback circuits, metabolic, transcriptional, and epigenetic responses that are responsible for "cell states," and is further complicated by the stochasticity of biochemical reactions. This high complexity of integrated pathways paved the road for developing more complex phenotypic screening, where changes in one or many cellular features become a measurable activity of a perturbagen, which can be described via the collection of hundreds to thousands of descriptors per cell (and organelle). In a broad sense, perturbagen-induced phenotypic changes refer to any modification in the "cell state," that can include cell morphology (*e.g.,* shape, texture), cellular contents (*e.g.*, protein, RNA), organelles, secretome, etc., and can be reproducibly measured, either in fixed samples or in live cells. The method of choice, by no means exclusive, that will be highlighted in this review is high throughput microscopy (HTM) coupled with image

Abbreviations: AI, artificial intelligence; CNNs, convolutional neural networks; CRISPR, clustered regularly interspaced short palindromic repeats; DAPI, 4′,6-diamidino-2-phenylindole; DCNNs, deep convolutional neural networks; DMSO, dimethylsulfoxide; DNA, deoxyribonucleic acid; EC_{50}/IC_{50}, half maximal effective/inhibitory concentration; ECM, extracellular matrix; EMD, earth mover distance; ER, estrogen receptor; FACS, fluorescence-activated cell sorting; FISH, fluorescence *in situ* hybridization; FOV, field of view; FRET, fluorescence resonance energy transfer; GANs, generative adversarial networks; GMM, Gaussian mixture model; GREB1, growth regulating estrogen receptor binding 1; gRNA, guide RNA; HiFENS, high throughput FISH detection of endogenous splicing isoforms; hiFISH, high throughput DNA FISH; HT, high throughput; HTM, high throughput microscopy; HTS, high throughput screening; JUMP, joint undertaking in morphological profiling; LINCS, library of integrated network-based cellular signatures; MAD, median absolute deviation; MERFISH, multiplexed error-robust fluorescence *in situ* hybridization; MOA, mechanism of action; ORF, open reading frame; PCA, principal component analysis; PDX, patient-derived xenograft; PROTAC, proteolysis targeting chimera; qPCR, quantitative polymerase chain reaction; QSAR, quantitative structure-activity relationship; RNA, ribonucleic acid; RNAi, RNA interference; RNA-seq, RNA sequencing; ROS, reactive oxygen species; TCCS, theta comparative cell scoring; XFP, x fluorescent protein.

* Corresponding author at: Department of Molecular and Cellular Biology, Baylor College of Medicine, Houston, TX, USA.
E-mail address: stossi@bcm.edu (F. Stossi).

https://doi.org/10.1016/j.bcp.2023.115770
Received 1 June 2023; Received in revised form 23 August 2023; Accepted 25 August 2023
Available online 1 September 2023

analytics. For details on instrumentation and software platforms supporting these types of studies, we suggest consulting these reviews [1–5].

Imaging allows for the fastest, and often least expensive, single cell analysis with the added benefits of multiplexing and spatial/temporal information (*i.e.,* inter-cellular relationships, organelle/intracellular organization). While it is challenging to use phenotypic screening to directly identify mechanisms of action (MOA) of any perturbagen, there have been several attempts to do so (*e.g.,* [6–16]), with various degrees of success. Overall, orthogonal, non-imaging-based assays should be employed to directly address the perturbagen MOA following selection as an active hit in a high throughput (HT) phenotypic assay.

Imaging and cell-based assays can be designed to report on multiple features simultaneously, which is a big advantage in terms of cost/benefit in large screening campaigns; moreover, the target does not need to be known *a priori*, may not have available *in vitro* assays or specific reagents, or the phenotypic change may only be measured in a living cell. In this experimental arena, unbiased image-based phenotypic profiling allows the generation of single cell-based, multidimensional "barcoding" for each perturbation of interest, whether based in a genetic or pharmacologic context.

2. Phenotypic heterogeneity and its use in high throughput screening

Cell-to-cell variation is an important feature in all basic physiological processes, from cellular differentiation to organ development, but also for single cells to sense, respond and adapt to environmental cues in a non-homogenous pattern [17–19]. The consequence of cell-to-cell variation in responses is reflected, for example, on the fact that cells do not respond similarly to drug treatments ("fractional killing", [20,21]), or that transcriptional responses are different at the cell- and allele-level (*i.e.,* [22–25]). To further complicate matters, protein dynamics at the individual cell level has been elegantly shown to affect drug responses [21].

Every biological system is intrinsically heterogenous (*i.e.,* cell-to-cell variation, organism-to-organism variation) which complicates analyzing the responses to perturbagens. It is well accepted that samples from different patients, or even when collected from the same patient (*i.e.,* two biopsies from two parts of the tumor), can have multiple phenotypes (and genotypes) and respond differently to a treatment. Consequently, personalized medicine has gained significant appeal, despite the additional challenges it presents in identifying new drug regimens, small molecule inhibitors, and their combinations. Fortunately, the emergence of rapid and scalable HT microscopes coupled with artificial intelligence (AI)-driven image analytics is turning the concept of large-scale personalized medicine into reality. These advancements hold immense promise and are poised to become the predominant approach for conducting chemical and genetic screens in the future. This transformative technology will not only revolutionize medicine but also find applications in other domains, including environmental toxicology [3,26].

At the same time, even simple isogenic models (*i.e.,* cancer cell lines) have a wide range of variation in every measurable parameter [27–33], a fact that is highlighted and readily quantified by imaging and analysis [34–36]. A recent outstanding review on single-cell techniques aimed at studying cell-to-cell variation can offer readers a comprehensive overview of this topic [37].

Most HTS studies report data as averages of the measured end point metrics over the cell population, which has similarity to traditional methods like qPCR, Western blot, luciferase reporter assays etc., which are usually easier to interpret and visually represent. However, our group and others clearly showed that intracellular signaling, protein levels, metabolic responses, and modulation of gene expression are often not uniform across a cell population (Fig. 1); and, perhaps more intriguingly, imaging-based single cell analysis has been used to identify rare cell states or drug resistant subclones [7,15,22,30,32,38–40]. Due to the capability of HTM to capture thousands to millions of cells in a single run, in a reasonable time frame, the term "deep imaging" has been used to identify studies of rare cellular events or subpopulations that have biological significance that are usually missed by population averaging [40–43].

2.1. How to measure phenotypic heterogeneity

All biochemical screening and most imaging-based approaches ignore phenotypic heterogeneity and assume that the distribution of the response to a perturbagen in a population is normally distributed across all measured features (*e.g.,* it follows a Gaussian distribution). However, this assumption may not hold true for many biological responses, famously cell cycle analysis, as can be easily seen by flow cytometry and also replicated by DAPI staining and imaging [44,45]. It is quite common to encounter multimodal and skewed distributions, particularly when considering on/off switches in cell signaling pathway

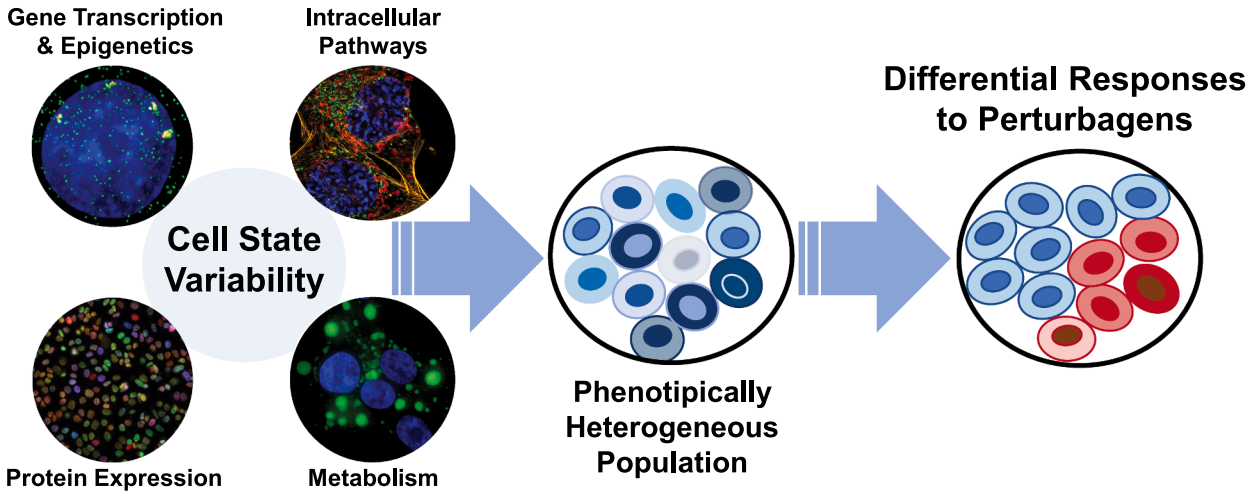

Fig. 1. Phenotypic heterogeneity can be described as the combination of individual cell variation in its "cell state" which derives from differential gene transcription and protein expression, epigenetic landscape, intracellular pathways, metabolism etc. This intrinsic variability of the cellular state causes differential responses to perturbagens (*i.e.,* drugs, environmental toxicants, metabolites).

[7,31,32,46–48]. Fig. 2 describes some of the metrics that have been used to measure phenotypic heterogeneity and that are discussed in more details next. Pioneering studies using image-based, single-cell analytics to query phenotypic heterogeneity were from the Altschuler group [7,47,49] where a panel of antibodies for selected pathways was used to extract dose–response effects of small molecules using single cell-derived distribution of features. They elected to use Kolmogorov-Smirnov non-parametric statistics as they recognized that cells in a well constitute a variable population due to being in different "states" (*i.e.,* phase of cell cycle, for example), and that the feature distribution was not normal. Similar ideas followed in other studies where the goal was to identify subpopulation responses by using a Gaussian Mixture Model (GMM) after data dimensionality reduction by Principal Components Analysis (PCA) [47,48,50].

Another approach to measuring phenotypic heterogeneity and use it for quality control of HTS campaigns was used by Schurdak and Taylor [31,32,46]. They applied several quality control metrics to validate responses on screening campaigns and applied them to describe single cell data heterogeneity after high content analysis. The chosen metrics were quadratic entropy (describing cell state diversity), Kolmogorov-Smirnov distance (a non-normality index for cellular subpopulations), and percent outliers (to identify the few cells that respond differently). Ultimately the three indexes were combined into a decision tree that allows researchers to classify the cell population responses into homogeneous, micro- and macro-heterogeneity.

More recently, we proposed an alternative method, corroborated also by other groups [45], that can be used for both quality control of single cell high content features and to characterize responses to perturbagens by analyzing the full distribution of single cell data, and measuring the earth movers distance (EMD) between distributions [30]. Interestingly, in this estrogen receptor-based study, we demonstrated that the distribution of this central transcription factor within a cell population was reproducible across multiple biological experimental replicates (>30); indeed, this approach indicated that phenotypic heterogeneity can be used as a stable metric for quality control of HT imaging campaigns. Furthermore, we were able to identify hits which would be defined as having a single cell distribution that is distant from a reference distribution (*i.e.,* DMSO control wells). We are currently expanding these observations to the multidimensional domain afforded to us by unbiased methods like Cell Painting [8,45,51,52].

3. High throughput microscopy assay development and applications

HTM screening campaigns have been used in many research areas including infectious diseases [53], cancer [54], genetic diseases [55,56], environmental toxicology [57–59], QSAR [60,61], PROTACs [62], and others (reviewed in [3,63]).

The primary objective of phenotypic, image-based perturbagen screening assays is to generate physiologically relevant and

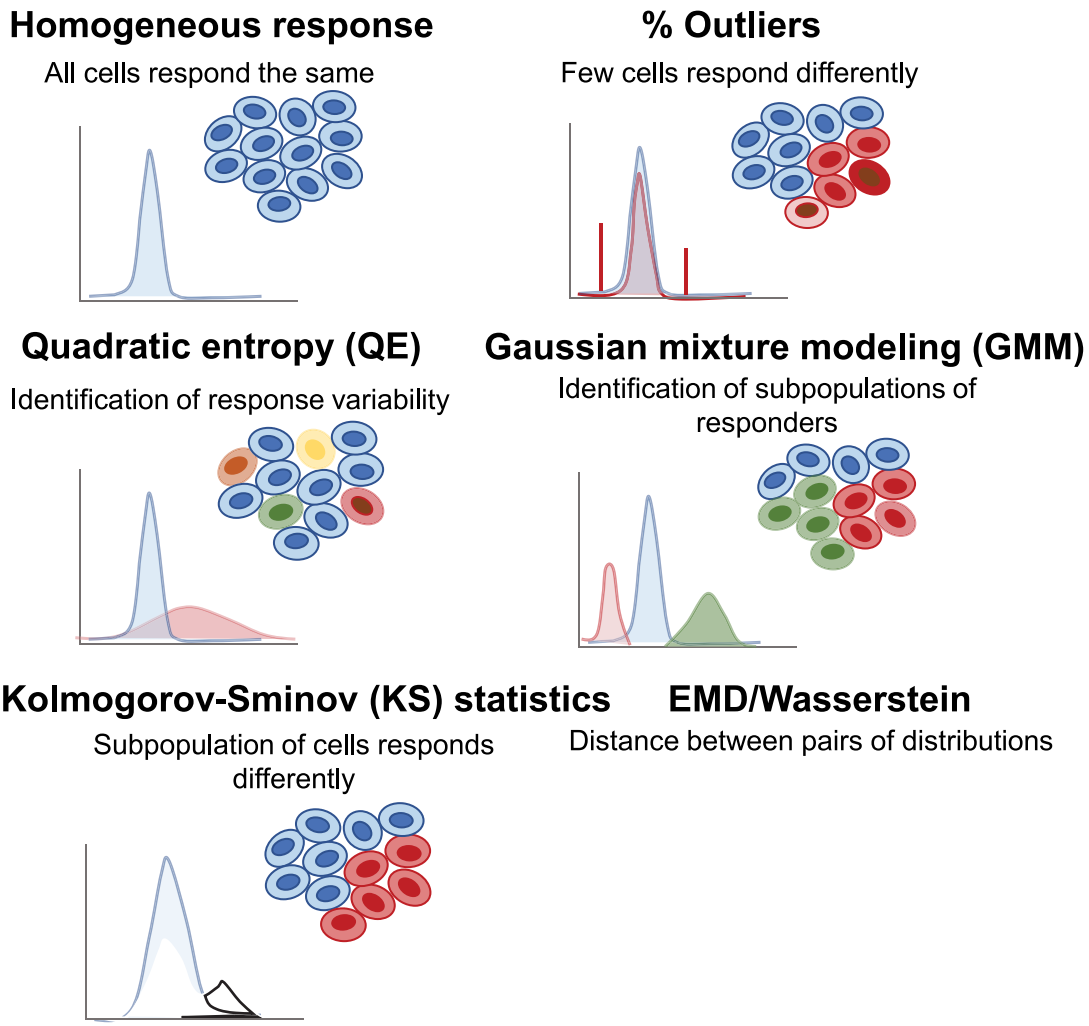

Fig. 2. Visual description of single cell-based metrics used to describe phenotypic heterogeneity of a cell population and its responses to perturbagens.

interpretable results. In the case of drug screening, these assays enable a more confident selection of high-quality hit compounds to further investigate. Furthermore, phenotypic assays demonstrate excellent reproducibility and sensitivity, making them valuable for analytical testing of various substances such as environmental toxicants, bacterial products, and supplements. To enhance the physiological accuracy of these assays, the utilization of tissue-mimetic models is preferred, as they can provide information that is closer to *in vivo* physiology. This approach, however, comes at the expense of higher reagent/labor costs and a reduced throughput. Nevertheless, efforts have been made in this direction, resulting in the development of complex 3D models, co-cultures, and engineered tissues and organs-on-a-chip, which will be discussed in Part 4.

3.1. High throughput microscopy (HTM) workflow

The typical workflow for medium- to large-scale HTM experiments includes the need for robotic liquid handling platforms (for cell plating, treatments/genetic modification, plate processing) and HTM, followed by the required computational/data storage resources for data handling and analysis (Fig. 3).

Depending on assay needs and design, widefield or confocal HT microscopy can be considered, usually with reflection-based (for speed) and/or image-based (for uneven cultures/3D models) focusing to acquire 2D (single focal plane) or 3D (z-stack) information. The number of field of views (FOVs) and z planes to acquire will depend on speed requirements, the robustness of the phenotypes measured (*i.e.,* if rare events or subpopulations need to be measured then a larger number of FOVs and replicates per condition will be needed), data analysis pipelines, and the availability of data storage. For imaging 3D structures (>~30 μm and <~300 μm in thickness), a spinning-disk HTM is often the preferred instrument as it allows speed through camera-based acquisition that is coupled with confocality to better capture information in the axial dimension. If a widefield instrument is used, the use of deconvolution algorithms should be considered to reduce the impact of out-of-focus light in images to be analyzed.

One of the critical choices for these types of experiments is the optical spacing during acquisition (*e.g.,* frequency of acquisition in the z dimension); however, this parameter can greatly increase the number of images acquired and may not be necessary depending upon the end point to be studied. To reduce the number of images and streamline analysis pipelines, the axial dimension can be collapsed into a 2D image by maximum intensity projection which is routinely sufficient for hit calling during HT screening campaigns. Obviously, by doing so, the captured spatial and structural cellular 3D information is lost. Moreover, maximum intensity projections skew the total intensity profile of the object as it only selects one intensity value per XY position, resulting in an underestimation of all intensity-based measurements. To optimally image large and dense structures, other steps might be needed, including refractive index matching, clearing, or expansion microscopy, all of which increase experimental workflow complexity, number of steps, and assay costs. Newer microscopy techniques offer the potential for enhanced speed and throughput in imaging large structures (*e.g.,* light sheet, [64,65]).

To make educated choices of all the parameters discussed above and assess the impact of each parameter on the metrics used to define perturbagen responses, it is necessary to conduct multiple trial runs.

The first step in high content assay design (Fig. 4) is to choose an available model that best-reflects the biological question(s) of the investigator and has the highest relevance; further, the assay must be amenable to imaging end points with practicality for scalability to robotic processing and large screening campaigns.

The second step is to decide the experimental end point(s) and how to detect it/them. In general, several approaches can be considered: 1) use of dyes for specific organelles, structures, biological response (*i.e.,* DAPI, annexin V, mitotracker etc. [51,66,67]), 2) use of mechanism-specific reagents (*i.e.,* antibodies, FISH probes etc. [7,22,49,68]) or, 3) use an engineered model with biosensors or reporters (*i.e.*, XFP-fused proteins, transcriptional reporters, FRET-based biosensors etc.). In many cases these methods can be combined, the number of parameters dependent upon the available imaging platforms, with 4–5 fluorescence channels being the norm. It is important to remember that reagent validation is paramount to the success/interpretation of HTM screens, especially if antibodies/probes are used, but also if XFP engineering is involved, as protein localization, functionality and dynamics can result in altered activities when compared to endogenous proteins [69–71].

The choice of the materials needed for the assay greatly influences the cost/well and labor time of the assay – for example, antibody-based multiplexed screens [49] or special techniques including single molecule RNA FISH [72], or DNA FISH (68) that are both markedly more expensive.

Next, the proposed assay needs to be miniaturized to reduce cost/well and to increase the real estate for screening small molecules in dose–response (and/or time), and/or genetic manipulations. Usually, in

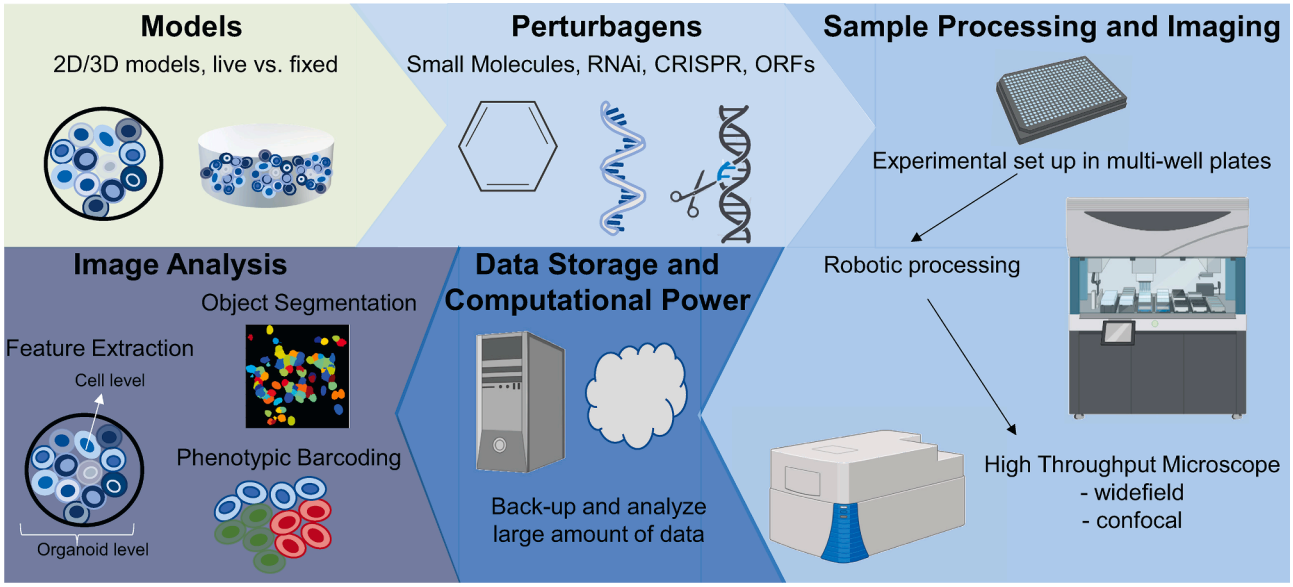

Fig. 3. Steps to consider for an efficient high throughput microscopy-based screen workflow.

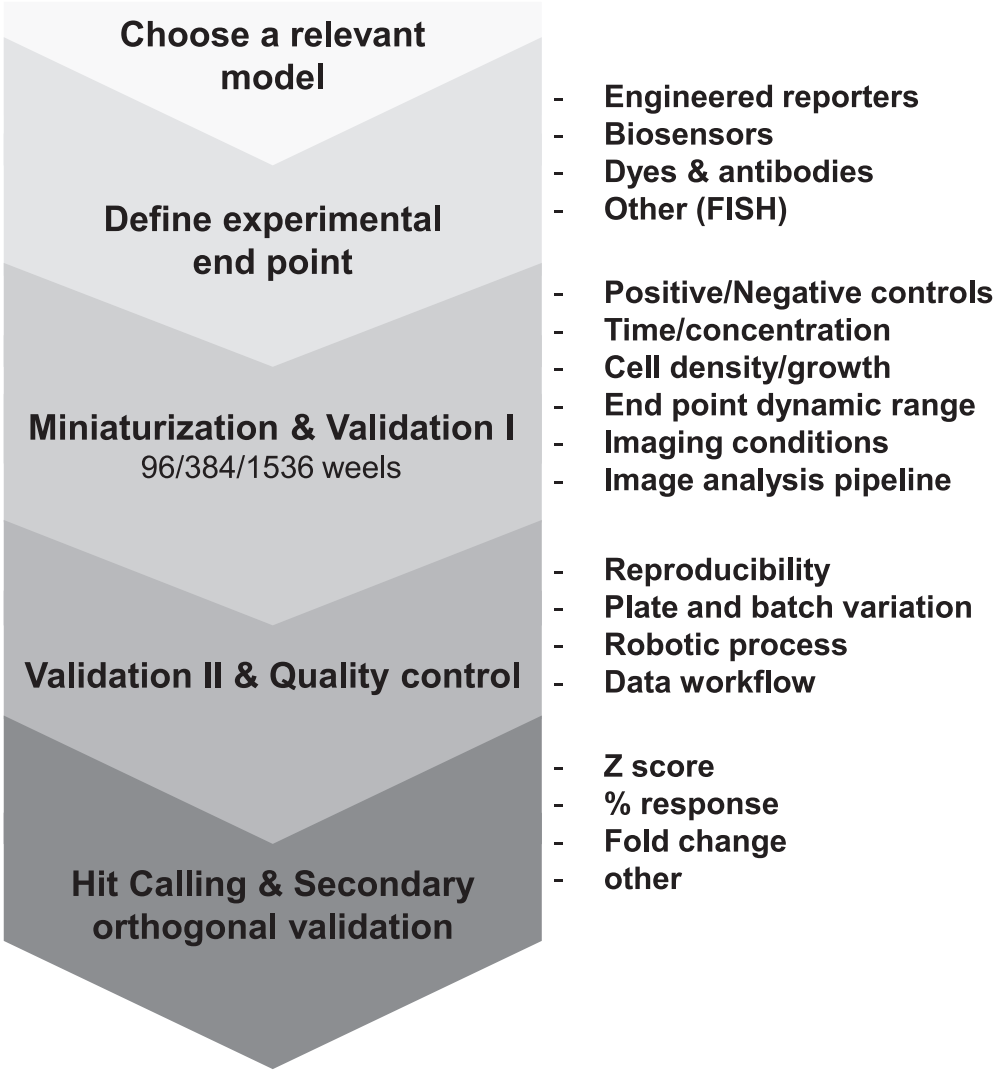

Fig. 4. Main steps that require evaluation and validation to perform a successful high throughput microscopy screen.

an academic setting, the preferred formats are 96, 384 and 1536 imaging-compatible well plates (either glass or optical plastic bottom, depending on the model studied).

Some of the parameters that need to be optimized before starting a screening campaign include: cell density, volumes, plate-to-plate and in-plate variability, batch effects, time of treatment, treatment concentration range (one vs. multiple), microscope type and imaging conditions, sample processing steps, analysis pipelines, required reagents and their available quantities, evaluation of toxicity parameters, and cell growth parameters for the duration of the assay. As one would expect, positive and negative controls for end point metrics of interest are required to accurately quantify the dynamic range of the assay and its reproducibility.

For medium/large HT campaigns, the introduction of multiple positive and negative control wells in different positions of each assay plate is necessary in order to avoid bias from edge effects and other non-biological variables, including robotic processing when staining/immunolabeling protocols are employed, and non-optimal imaging parameters [45,73]. Ideally, for each screening campaign there should be two sets of reproducibility controls: both technical and biological controls are essential. Each perturbation should be detectable in several wells per screening campaign to ensure reproducibility of the effect; this could be done using several wells on the same plate or by creating replica plates. Often the choice or the strategy and number of technical replicates depends on the strength and reproducibility of the expected effects, cost, robotics capabilities and other practical considerations. In terms of biological replicates, the choice also depends upon the strength and reproducibility of the positive control.

The most traditional way to evaluate the performance/robustness of an assay, when only one end point/well is measured, is the Z prime score (Z', [74]) that takes into account the dispersion of the negative and positive controls and their separation (*i.e.,* dynamic range of response). However, for single cell analysis, subpopulation analysis, co-cultures, and 3D organoids, including multi-dimensional image analysis, this method is not well suited since biological variation is often too large to pass this classic quality control test (usually Z'>0.5 is needed for an assay to be usable in screening campaigns). For this reason, new metrics for quality control have been recently proposed. In particular, both our group and others have been exploring new avenues to use single cell data extracted from the images and feature distributions to define quality control metrics for HT campaigns based on phenotypic heterogeneity [30–32,39,46].

To obtain comprehensive guidelines for assay development, the reader should refer to the excellent NIH-supported e-book on HTS [75]. This valuable resource covers a wide range of topics, including a newly added chapter dedicated to image-based screening [73]. Additionally, the reader can explore other extensive reviews that delve into various aspects of assay development [15,26,76,77].

After the primary screening campaign is completed and hits have been called, they will need to be validated through several potential follow-on approaches. For example, by acquiring a different commercial source of the hit chemical or a new synthesis batch when prepared in house, by performing extended dose-responses to calculate the EC_{50}/IC_{50} (half maximal effective concentration/inhibitory concentration) values, and, more importantly, use of an orthogonal assay that has a different method of detection as the imaging-based primary screen (*e.g.,* luciferase reporter, qPCR for target genes, Western blot for protein levels, etc.); with the ultimate goal being comprehending the mechanism of action of the perturbagen before moving into more complex systems (*i.e.,* HTM-compatible model organisms).

4. Image analysis and data visualization

Image analysis plays a critical role in extracting meaningful biological information from large number of images that typically encompass multiple structures spanning a wide range of scales. To handle the overwhelming volume of images acquired through HTM and assist biologists in the interpretation of data, automated image analysis pipelines have been introduced to aid in the quantification and interpretation of thousands of images [4,5,78–82]. As several hundreds to thousands of numerical features can be extracted for each cell comprising a multiplicity of feature types (*e.g.,* intensity, shape, texture), the analysis, interpretation and visualization of these data requires the use of advanced image processing methods, including statistics, machine learning, AI etc. These strategies align with those employed by other multidimensional omics technologies like proteomics and transcriptomics.

The fact that it is possible to extract a myriad of metrics per cell has evolved into the concept of "high content" analysis, dating back to the late 1990s [83], and is currently one of the most common ways to describe image-based multiparametric analysis. Automation is crucial at every step of the analysis to facilitate HTM screens. With thousands of wells and many thousands of cells to be analyzed, automating these processes becomes imperative to accomplish the task within a reasonable timeframe.

A typical image analysis pipeline (Fig. 5) for morphological high content screening includes: (A) a preprocessing step to improve image quality and facilitate subsequent processing steps; (B) a segmentation routine to accurately/efficiently identify objects of interest (*e.g.,* cells, nuclei, other cellular landmarks); (C) a quantitative feature extraction routine to collect information from segmented cellular structures; and (D), a feature selection and analysis routine that facilitates to identify the most relevant features followed by a final processing step of (E) phenotypic barcoding and hit calling. We will describe further below how each step may be carried out and review current state-of-the-art implementations, and their technical challenges.

Preprocessing may include separate routines to correct for uneven illumination, eliminate out-of-focus FOVs, and flag and remove FOVs with evident artifacts etc. Numerous algorithms have been suggested for illumination correction of images in HTM [84]. Nevertheless, the significance of preprocessing has diminished in recent image processing pipelines compared to the past. This change can be attributed to the shift from pixel-based methods, which are highly sensitive to image intensity and contrast (*e.g.,* intensity thresholding), to incorporating current image processing pipelines using learning-based methods that are considerably more resilient to image noise and contrast.

Image segmentation has the goal to identify individual cells and other subcellular structures that may include nuclei, organelles, and more. This is often the most challenging processing step of image analysis as most biological samples offer extensive phenotypic variability (large variations in shape, size, and contrast), thus making accuracy a difficult problem to solve. The segmentation task can be further complicated by the projection of information occurring over multiple z-sections into a planar image, causing potential distortions. State-of-the-art methods for

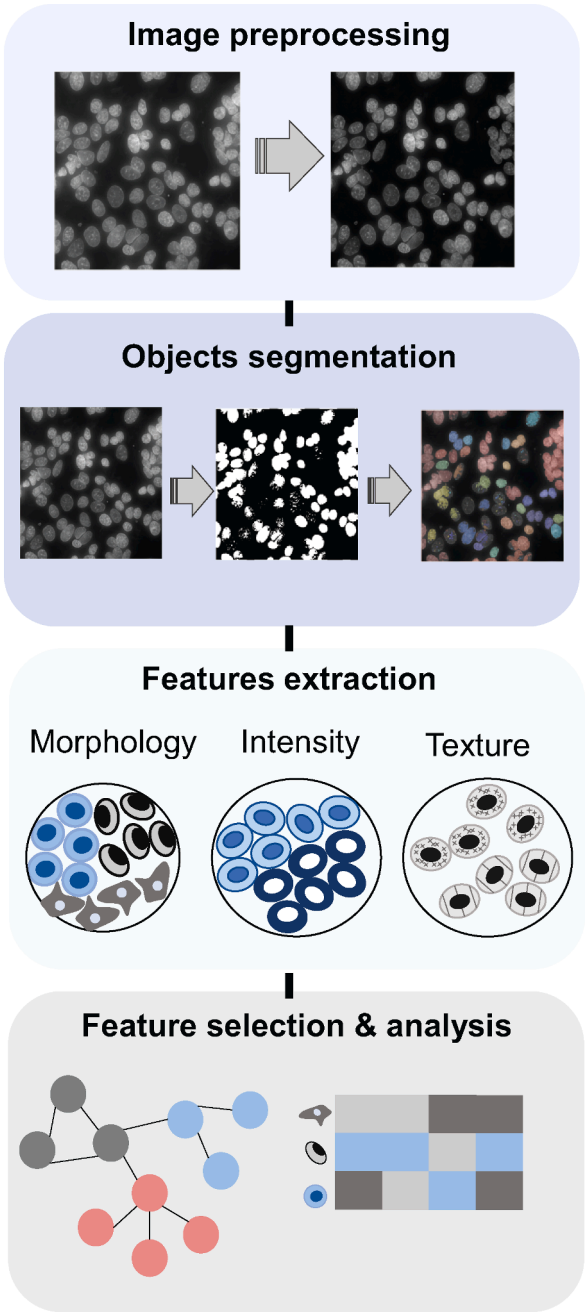

Fig. 5. Typical image and data analysis workflow.

cell segmentation are based on deep convolutional neural networks (DCNNs) and provide results that are significantly more accurate and reliable than conventional algorithms based on morphological operators or variational methods. However, as for any learning-based approach, DCNNs require manually annotated datasets for training and their performance tends to decrease when applied to images that appear fundamentally different from anything observed during training. Collectively, it is fortunate that advances in this active area of research and the increased availability of annotated biological image data sets from open-source repositories have made it possible to develop a new generation of deep learning cell segmentation algorithms, such as *Cellpose* [85], that includes large ensembles of diverse, pretrained models that can accurately segment a wide variety of cellular images.

Feature extraction is applied at the single cell level to collect quantitative information that can be used to reliably discriminate among different cell types and conditions. Collected features are numerical

values describing several cell characteristics, including fluorescence intensity, shape, geometry, and textural properties. To facilitate feature computation, several open source and freely available feature libraries have been created, such as pyradiomics [86], the libraries contained in *scikit-image* [87], and open CV [https://opencv.org/] repositories – each library containing several hundreds to over a thousand possible features. We would also like to mention the popular CellProfiler image analysis software [88] that includes a large library of size, shape, intensity, and texture features targeted to HT cell analysis. We remark as features are computed using the cellular and subcellular masks obtained from the segmentation stage, inaccurate segmentation can affect feature computation that can introduce significant errors. This observation highlights the importance of the segmentation step and identifies a major limitation during feature extraction *e.g.,* its sensitivity to segmentation errors. We remark that feature normalization is also an important step of feature computation due to the need to compensate for plate-to-plate variations and to have all features at the same scale to simplify subsequent steps of analysis/visualization. The most common way to do so is to utilize the untreated control wells as the baseline; next, for each feature, to subtract the median and divide by the MAD (median absolute deviation) of the control wells [45,73,89].

Feature selection is designed to prune the features by selecting the most informative, those that are most effective at discriminating different cell types and conditions and are also more reproducible in separating diverse phenotypes. This task can be achieved through several data reduction methods, including covariance matrices, principal component analysis (PCA), and machine learning, when training data sets are available [45,49,73,79,90,91].

Feature normalization is also needed to compensate for plate-to-plate variations and to have them all in the same scale to simplify subsequent steps of analysis/visualization. This is most implemented utilizing untreated control wells as baseline. Then, for each feature, the median can be subtracted and divided by the MAD (median absolute deviation) of the control wells.

Phenotypic barcoding and hit calling. Following feature selection, all features are summarized as a "phenotypic barcode" for each well or cell so that the different perturbagens (chemical, genetic, etc.) can then be ranked in terms of their hit-calling activity. The most representative assay that exemplifies phenotypic barcoding is Cell Painting [8,51]. The Carpenter group provided a study comparing several phenotypic profiling methods that emphasized small molecule mechanisms of action [92]. Their approach included the mean taken over all scaled features [51], Kolmogorov-Smirnov statistic [7], support vector machine hyperplanes [49], Gaussian mixture models, and factor analysis. An additional phenotypic barcoding idea is the Theta Comparative Cell Scoring (TCCS) method that was developed by the Carragher group [93,94] and applied to Cell Painting assays across multiple cell models. An interesting aspect of this method is that it can be used across omics platforms to integrate more information about the MOA of a specific perturbation. To quantify differences between profiles, several methods have been used that include the use of a similarity index [9], Mahalanobis distance [12], Euclidean distance [6,62], grit score (https://github.com/broadinstitute/grit-benchmark, [62]), hierarchical clustering etc.

5. High throughput assay types applicable to phenotypic screening

In this section, we present several examples of HT assays (Fig. 6) that have been conducted using imaging as an endpoint, with a particular emphasis on 3D models. At this juncture, not all these approaches have been employed for phenotypic analysis, but the trend to do so is evident and we anticipate they will gain greater prominence in the near future.

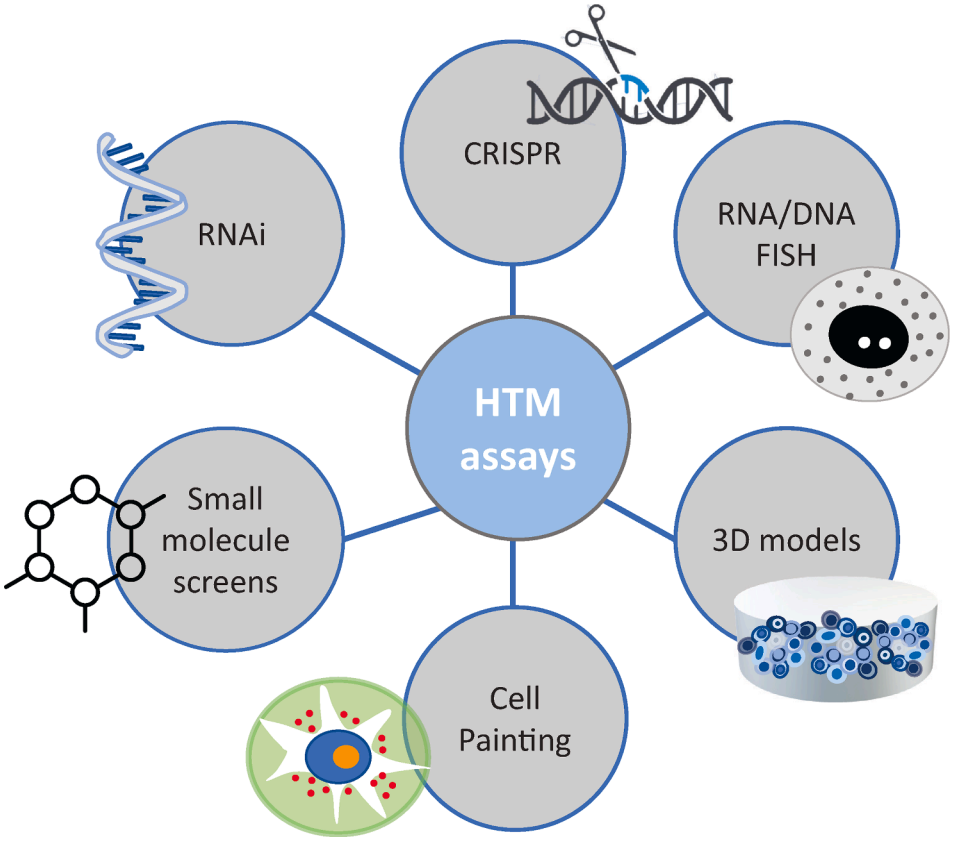

Fig. 6. Overview of the types of assays that have been employed in high throughput microscopy.

5.1. Small molecule screens (investigational compounds, drugs, environmental toxicants)

The most common way of performing an HTM screening campaign, similarly to other methodologies, is by treating the model system with various size libraries of chemical compounds from natural or synthetic sources (for examples see [6,12,55,56,58,95–101]), and measuring selected end points. While cell death and cell health are commonly used as endpoints, there is a growing recognition of the significance of phenotypic changes, including alterations in morphology and protein levels. These phenotypic changes provide more comprehensive insights into the mechanism of action of a perturbagen including potential off-target effects.

The compound libraries available to screening centers vary in size from a few hundreds to a few million chemical moieties that are organized in focused collections of specific target classes (*i.e.,* kinases, epigenetics, etc.), or aim for the largest chemical diversity. Also, libraries are available comprised of molecules that have been tested in humans (which speeds up then bench-to-bed side timeframe), or on completely developmental moieties to explore wider chemical spaces, including those that are of natural origin.

Especially for phenotypic screening (*i.e.,* Cell Painting or similar), where the readout is not necessarily linked to a single mechanism of action, it is useful to characterize the effects of small molecules by defining a quantitative "fingerprint" through the combination of the multidimensional descriptors obtained via image analysis. Examples of such attempts [7,8,102–106], link phenotypic changes to drug sensitivity and drug resistance. A powerful example can be found in [54], where the authors use an imaging-based phenotypic assay, labeling only DNA and actin, in order to profile>1200 compounds in twelve isogenic cell lines containing mutations in key oncogenic pathways.

In HT screening campaigns, it is important to have detailed annotations of the library compounds to better-enable interpretation of results used to predict mechanism of action of novel moieties [61,107], and ultimately to integrate results with other omics, notably transcriptomics. For example, identifying false positives upfront (*i.e.,* toxic compounds, when this is not an assay end point) can help reduce the number, cost, and time of follow up experiments required to determine an unwanted mechanism of action. Interestingly, a new study from Dahlin et al., [66] approached the problem using a HT Cell Painting scheme to identify compounds with unwanted characteristics (*i.e.,* toxic or causing cellular damage) that can be used as references in larger screens.

5.2. Genetic screens (RNAi, CRISPR, ORF)

Alternatives to small molecule testing are genetic screens using most commonly RNAi, CRISPRs or ORF overexpression. These types of approaches allow for connecting the effects of modulating specific genes to cellular phenotypes of interest, either mechanistically or in an unbiased manner.

HT RNAi screens have been used to dissect basic mechanisms of cellular responses, states and subcellular structures, including stress granules [108], nucleoli [109], Golgi [110], mitosis [111–113], endocytosis [114–116], DNA damage response and genome instability [117,118], autophagy and mitophagy [119,120], and others (*i.e.,* [121,122]).

As CRISPRs become a more-widespread tool, they will supplant RNAi screens as they have been shown to be able to have a higher hit rate and easier interpretability [123,124]. Moreover, RNAi relies on transfection methods that do not guarantee uniform down-regulation of the target in each cell and is prone to off-target effects; however, this can be somewhat mitigated by the use of multiple RNAi probes targeting the same RNA, and also by analysis of single cell distributions of the assay endpoints.

CRISPR screens (Fig. 7) are performed using either arrayed (*i.e.,* one gRNA/well) or pooled guide RNA (gRNA) libraries, where identity of the hits is discovered by sequencing sgRNA *in situ*, or following FACS sorting and sequencing. For readers interested in a more comprehensive review of recent methodologies in this space we suggest Lawson and Elf [125].

Some recent examples coupling CRISPR and imaging can be found in [126–128]. For experimental details, setup, and analysis of CRISPR high content screening, including specialized imaging-based screens, please consult Bock et al., 2022 (https://www.nature.com/articles/s43586-021–00093-4).

Arrayed gRNA libraries are especially advantageous when coupled with HTM as phenotypic changes, measured either by pathway specific reagents or in an unbiased manner through Cell Painting, can directly be

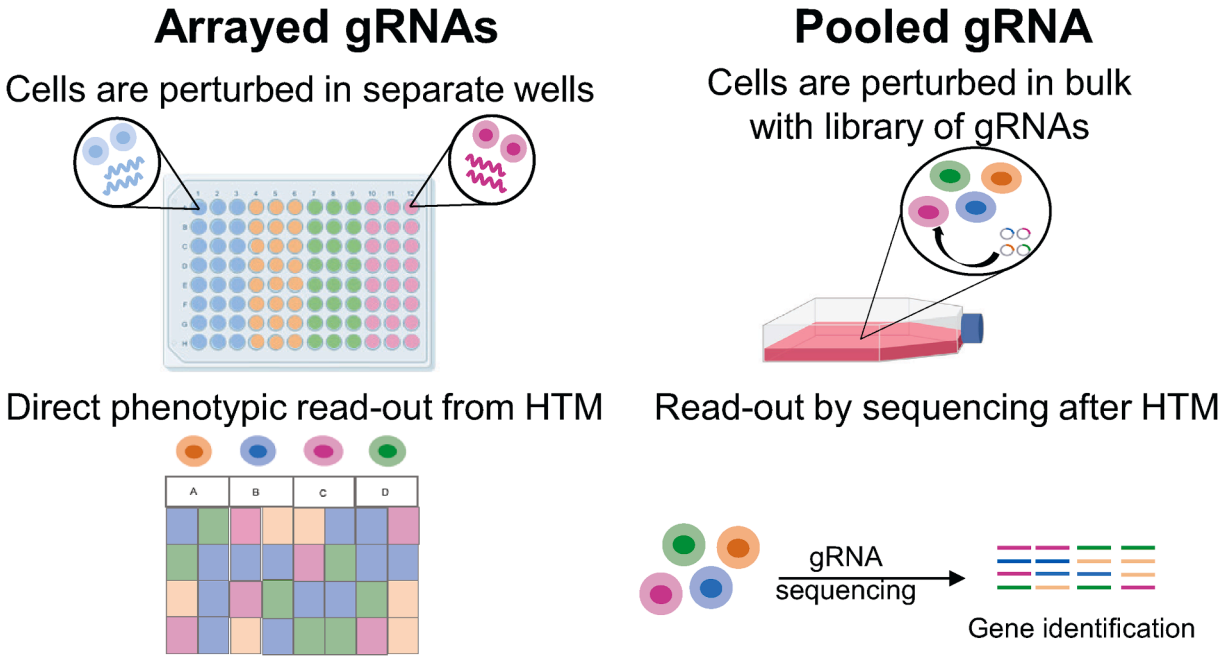

Fig. 7. Comparison between two CRIPR-based screening modalities that have been combined by high throughput imaging.

related to the gRNA spotted in a specific well [77,128–130], however, they require a many more plates for each experiment thus increasing the relative cost/well.

Novel methodologies have also been employed that link HT imaging with pooled gRNA libraries, for example through the use of microRaft arrays to isolate clones for sequencing and hit identification [131], or photoactivation/photoconversion of hit cells for subsequent FACS isolation and sequencing of sgRNAs [124,126,132].

More recently, Funk et al., [133] published a resource paper where the authors identified essential genes in HeLa cells that modulate cell phenotypes by screening > 20,000 sgRNAs against > 5,000 target genes, successfully combining a CRISPR pool screening with HTM, where cells were labeled to measure DNA content, DNA damage, actin, and microtubules.

More complex imaging-based methods such as MERFISH, which couples multiple rounds of fluorescence *in situ* hybridization (FISH) to analyze specific barcodes by imaging, have also been performed in combination with CRISPR screens [134]. However, the scalability of such methods to HTS will require additional technological advances in order to become a cost effective and rapid tool for drug screening.

5.3. Unbiased phenotypic screening and Cell Painting

Unbiased analysis of changes in cellular phenotypes can be performed using methods similar to Cell Painting that use inexpensive dyes to label cellular structures [8,51,52]. This assay approach, or similar, with specific antibodies, have been used across many genetic modifications and small molecule treatments, and is being heavily utilized in drug discovery, environmental toxicology, QSAR, functional annotation of libraries of compounds and more, both in academia and in industry. Suggested examples on how Cell Painting has been applied in screens are now abundant [13,57–59,61,135–142]. The widespread adoption of phenotypic screening via Cell Painting has been certified by the establishment of the JUMP (Joint Undertaking in Morphological Profiling)-Cell Painting Consortium (https://jump-cellpainting.broadinstitute.org/) that brings together academia and industry to transform drug discovery by integrating HT imaging with emerging data mining technologies. The consortium is rapidly making significant progress, with initial analysis stages and datasets being made accessible to the public [89]. These resources are expected to serve as valuable assets for scientists worldwide, providing an extensive repository of information and facilitating groundbreaking research in the field.

Many variations of the canonical Cell Painting protocol have been proposed, notably using specific pathway/morphological antibodies [7] or dyes and combinations thereof. As an example, Way et al. [67] validated a suite of HT "cell health" assays to analyze 70 cell status indicators used to interpret effects of perturbating basic cellular functions, including cell cycle, apoptosis, ROS, DNA damage etc. Similarly, Howarth et al., [143] used live cell dyes to monitor various cellular states (*i.e.,* healthy, apoptotic, necrotic, etc.) followed by high content image analysis and classification of subpopulations.

5.4. RNA and DNA fluorescence in situ hybridization (FISH) in HTM screening

HTM screens using RNA or DNA FISH as end points are more complex and expensive as they require additional steps and reagents than classical assays, and are also difficult to automate (*i.e.,* RNAse free reagents, temperature shifts for incubation and washing, longer waiting times). Despite these challenges, there have been several attempts to improve the workflow and reagents used to perform such complex assays in high throughput mode. For example, Safieddine et al. [144] developed HT-smFISH, a more cost-effective way to perform 96-well based screens for analysis of a limited number of target RNAs/campaign. Interestingly, Dr Misteli's group successfully developed protocols for HT DNA FISH (hiFISH, (68,122)) and, more recently, for measuring splicing outcomes at endogenous genes using hybridization chain reaction (HiFENS, [145]). Our group has also contributed directly to this area by performing a small screen with epigenetic inhibitors that coupled estrogen receptor (ER) immunofluorescence with smFISH to a prototypical endogenous ER target gene (GREB1). This focused screen thus facilitated the discovery of a new cellular mechanism that controls the frequency of allelic activation of a hormone responsive gene [22]. Perhaps, more than being used in HT screening campaigns, these types of assays will provide a tool for pointed secondary screens and perturbagen mechanism of action evaluation.

5.5. 3D model systems in HTM screens

The field of drug discovery has recently witnessed a distinct shift towards evaluating chemical moieties and genetic modifications with increasingly complex and "physiological" models. This transition can be attributed to the continuous advancements in various technology domains, including HT imaging instruments, robotic handling systems, bioprinting techniques, biomaterials, and more. These developments have enabled researchers to explore and test compounds and genetic interventions within models that closely mimic physiological conditions.

The goal of 3D cultures is to generate models that more closely resembles real organs/tissues/disease states versus the classical 2D models growing on plastic, combined with lower cost, higher speed, and reproducibility, as compared with animal models (reviewed in [146]), although still being more expensive than traditional 2D assays (Fig. 8). Moreover, combining HT 3D screening with patient derived tumor models is paving the way for drug discovery coupled with personalized medicine [147–150]. Using organotypic multicellular developmental or disease models allows for characterization of perturbagens on specific cellular subtypes, different stages of development/disease, different time scales, etc., depending upon the biological or therapeutic question of the investigators. It must be remarked that not all end points that are available from 2D cell models can be recapitulated in 3D using current technology, notably nuclear translocation, organelle analysis, vesicle trafficking, RNA/DNA FISH, and more. Additionally, protocols that are easy to automate and perform in 2D HT screens must go through extensive validation steps including washing steps, treatment regimes, fixation, staining and immunolabeling, antibody penetration etc.

A standard assay upgrade is to grow canonical 2D cell models in 3D systems that more closely represent the *in vivo* growth and organization of the cells [151–157]; typically, this can be through either low attachment systems or embedding into extracellular matrixes (ECM).

The choice of ECM is a critical decision to consider in screening campaigns as it greatly influences the behavior and drug responsiveness of the chosen cell models, and especially the cost/well (*e.g.*, [158–160]). Both the composition of the ECM and the stiffness of the matrix can be used to mimic tissue specific effects that can change the effects of drug treatments/resistance [161–163].

Several methodologies have been developed and often adapted to HT microscopy for small and large chemical/genetic screens. Some of the major challenges are automation and reproducibility of 3D cultures (size, organization, different donors, lots of ECM etc.), and the added complexities associated with proper imaging of large 3D structure. It is worth noting that a key caveat to 3D assays can be lack of reproducibility, which is also enhanced by the difficulty of obtaining enough material (*i.e.,* primary samples, PDXs etc.) to perform the necessary replicates per condition. Further, as single cell analysis of a 3D structure is not yet mainstream, every spheroid is considered as one unit, greatly limiting the statistical power of the analysis (in comparison, 2D cell models analyze several thousand data points/condition at a single cell level).

3D cultures can be formed and grown in a miniaturized format either in scaffold-free systems that rely on self-aggregation (*i.e.,* hanging drops, low attachment plates, round/V bottom plates, magnetic levitation, etc.)

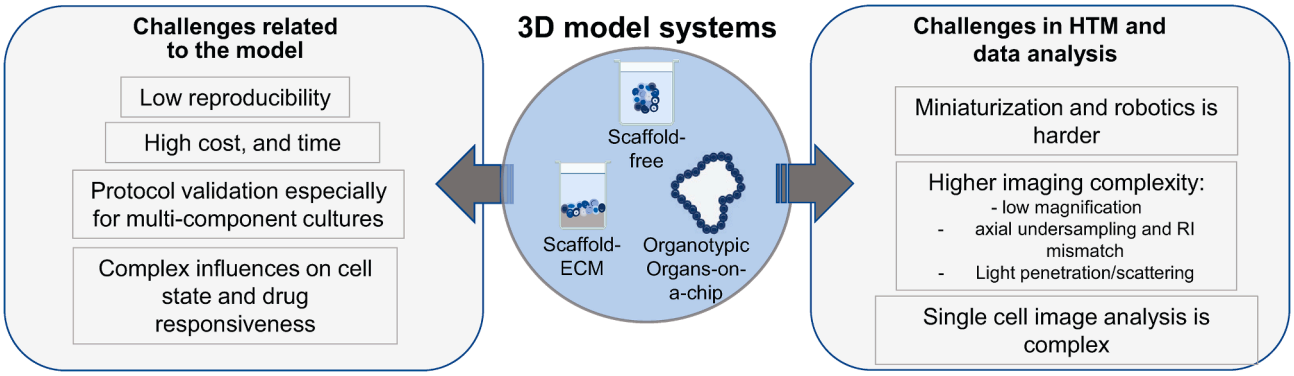

Fig. 8. Challenges in 3D models establishment, imaging, and analysis.

or encompassing a bio-compatible substrate, either of biological (*i.e.,* collagen, Matrigel®, alginate, gelatin etc.), or synthetic (polyethylene glycol, hyaluronan acid, etc.) origin.

For a comprehensive review on 3D culture methods, we refer the reader to [2,152,164]. An interesting technology that has been used in HTS involves magnetic levitation of cells that take-up non-toxic magnetic nanoparticles in order to rapidly create 3D spheroids [147,165,166].

Advancements in automation, microfabrication, and imaging instruments are paving the way for the expansion of imaging-based HTS to encompass more complex and clinically relevant model systems. These developments are bringing us closer to the realization of utilizing complex and realistic model systems in HTS applications. For example, Puls TJ et al. [167] developed a fully automated system to control ECM stiffness and build pancreatic cancer 3D spheroids for drug screening.

As the size of the 3D spheroids/multicellular organoids is variable, there are numerous challenges linked to imaging and image analysis that are constantly under development [168]. Most often images (brightfield and/or fluorescence) are captured with either widefield or confocal HTM using only low magnification/low resolution objective lenses (from 2.5x to 10x) with a set of under-sampled z-stacks to save time and data storage. One of the challenges the field will face in the coming years will be achieving isotropic HT imaging with single-cell resolution in 3D due to the inherent density of typical 3D spheroids, along with the presence of necrotic centers. This issue hinders effective light penetration and collection. Overcoming this challenge will necessitate the adaptation of alternative techniques (*i.e.,* clearing ([169]) and light sheet [170] for example) to enable comprehensive phenotypic analysis in a true 3D context.

The complexity of 3D models poses limitations in the type of features that can be currently computed and analyzed from each spheroid; the most commonly used are size and shape features extracted from brightfield images [150,171,172], or total fluorescence intensity from maximum intensity projections using dyes, antibodies, or engineered reporters [149,156,172–180] to measure cell health, apoptosis, or cell cycle. Some examples of translationally relevant 3D models that have been recently used in HT drug screening include prostate, colorectal, pancreatic, and other cancer types used in patient derived xenografts and primary tumor-derived cells [147–150,173,174], and also polycystic kidney disease models [181], cancer-stromal cell coculture [182], and patient derived glioma stem cells [175].

6. Future perspectives

6.1. Integration across data types (data fusion)

Integrating multi-level or multi-modal information content from several OMICs platforms and other data types (*i.e.,* chemical structures) has the promise to enhance drug identification, testing and personalized medicine, and is rapidly evolving. The most common integrations have been between classical bulk population OMICs techniques (*i.e.,* RNA-seq, proteomics, metabolomics), as it is more challenging to include single cell and imaging end points. As an example, Nassiri et al., [183] integrated the cellular morphological features with gene expression profiling performed by the LINCS project. More recently, a similar effort was performed by the Carpenter group integrating Cell Painting features with L1000 mRNA measurements clearly demonstrating complementarity of the two approaches [142]. Interestingly, adding chemical structure to imaging and gene expression features increased prediction of compound activity by almost three fold, further highlighting how fusing multimodal data has the potential to reduce time and cost in drug discovery [184].

6.2. Live imaging and label free microscopy: Adding the 4th dimension

Many of the experimental protocols described in this review can be adapted to live imaging, and indeed several have been performed on live cells. Additional complexities in performing live HT screens include phototoxicity, media evaporation, frequency and length of acquisition, data storage etc., all becoming important new factors to consider during experimental design and require extensive validation in pilot studies.

However, for highly dynamic or transient processes, or to follow specific cells or subpopulations over time, live imaging-based screens are necessary [185]. The easiest and more cost-effective way of performing such experiments is to engineer cells to express markers of interest, or pathways using biosensors/activity reporters. A good example of phenotypic HT drug screening study with engineered cell lines can be found in [6], where the authors created 15 reporter cell lines with multiple fluorescent markers combination against actin, endosomes, DNA repair, Endoplasmic Reticulum, mitochondria, Golgi, microtubules, autophagosomes, NFkB signaling, and clathrin. Another good example is the development of Dye Drop, a HT, customizable and automatable protocol that combines live and fixed cell imaging endpoints to enhance data content per screen [186].

Another solution that is constantly evolving in terms of throughput, instrumentation and software for single cell analysis and tracking, is to use quantitative label-free methods, most notably holo-tomography or quantitative phase imaging, which have very low to no phototoxicity, are in general much faster in acquisition and provide quantitative measurements at the single cell and organelle level by leveraging refractive index mapping [187–189]. An example of drug testing using label-free imaging can be found in [190].

6.3. Multi-cellular compartment models

As technology improves, the ultimate goal is to produce models that more faithfully recapitulate organ/tumor environments used in HTS [191,192]. Here, the hope is of adding multi-cellular compartments (*i.e.,*

stromal, and immune cell co-cultures) with, for example, tissue-like organization and stiffness, maintenance of oxygen and nutrient gradients to provide an optimal medium for drug discovery between 2D screen and animal studies. Even at the basic level of having two cell types in an assay, step of the experimental setup requires extensive validation, including cell type ratios and growth patterns, maintenance of the proper physiological responses etc. As with any 3D culture model, reproducibility will always be an issue. With bioprinting techniques becoming more and more popular, perhaps some of these hurdles will be mitigated by automation [193,194]. In addition, the new frontier in drug development is the generation and validation of organs-on-a-chip that have the potential to recapitulate *in vitro* most of the characteristics of *in vivo* models (for recent reviews on this topic see [195]). Due to cost, production, and complexity, it is unlikely that many of these systems will become a HT modality for even small screens; however, they should prove to be an excellent resource with higher predictive value as compared to animal models during the drug development process.

6.4. HTS and artificial intelligence

The impact of deep learning and artificial intelligence on emerging applications in high content screening is significant [26,80]. As mentioned above, in addition to improving image segmentation and other image processing tasks, deep learning models have been proposed for super-resolution and cross-modality image transformations in fluorescence microscopy [196]. These models utilize generative adversarial networks (GANs) that learn critical features from training data to generate high-resolution images from low-resolution inputs. This approach has the potential of increasing the use of larger imaging fields to increase the number of captured objects, improve image resolution under poor illumination conditions, and reduce the required number of frames and illumination, thus limiting phototoxicity in live experiments. The application of GANs for morphological profiling is equally promising. Generative methods can learn rich feature representations of cells and synthesize realistic images in 2D or 3D, enabling the exploration of morphological heterogeneity and variation in cells, and the evaluation of their mechanism-of-action classification performance [197].

Furthermore, deep learning enables the inference of relationships between visual phenotypes and chemical structures that can complement or replace assay predictions in virtual screens. For example, Zapata et al. [198] trained a deep learning model on high content images and associated morphological profiles to identify molecules that induce desired morphological changes. Similarly, Hofmarcher et al. [199] developed an end-to-end deep neural network to directly predict assays from images, eliminating the need for complex cell segmentation and feature extraction. Their work demonstrated that convolutional neural networks (CNNs) operating on raw images outperformed traditional feature-based methods, showing improved prediction power and efficiency.

However, a limitation of deep learning models is the lack of direct interpretation or biological meaning within the encoded feature maps, and during cell screening and profiling applications, it is crucial to interpret the patterns found in the data. Therefore, further research is necessary to develop deep learning architectures that are interpretable in a biological context. This includes the identification of positive and negative examples associated with a phenotype and the utilization of causal inference methods to understand the biological effects of interventions.

Nevertheless, the emergence of deep learning and artificial intelligence has brought transformative advancements to high content screening, and further developments in these areas hold the potential for even more significant and rapid impact.

CRediT authorship contribution statement

Fabio Stossi: Conceptualization, Writing – original draft, Writing – review & editing, Visualization, Funding acquisition. **Pankaj K. Singh:** Conceptualization, Writing – review & editing. **Kazem Safari:** Conceptualization, Writing – review & editing. **Michela Marini:** Conceptualization, Writing – review & editing. **Demetrio Labate:** Conceptualization, Writing – review & editing. **Michael A. Mancini:** Conceptualization, Writing – review & editing, Funding acquisition.

Declaration of Competing Interest

The authors declare that they have no known competing financial interests or personal relationships that could have appeared to influence the work reported in this paper.

Acknowledgments

This review was supported by the GCC Center for Advanced Microscopy and Image Informatics (CAMII) with funding from CPRIT (RP170719). We would like to thank Renata Mendonça Moraes for help with figure design and assembly. Some of the figures contain graphics from BioRender.com.

References

[1] L. Li, Q. Zhou, T.C. Voss, K.L. Quick, D.V. LaBarbera, High-throughput imaging: Focusing in on drug discovery in 3D, Methods San Diego Calif. 1 (96) (2016) 97–102.
[2] N.J. Martinez, S.A. Titus, A.K. Wagner, A. Simeonov, High-throughput fluorescence imaging approaches for drug discovery using in vitro and in vivo three-dimensional models, Expert Opin. Drug Discov. 10 (12) (2015) 1347–1361.
[3] S. Li, M. Xia, Review of high-content screening applications in toxicology, Arch. Toxicol. 93 (12) (2019) 3387–3396.
[4] J.C. Caicedo, S. Cooper, F. Heigwer, S. Warchal, P. Qiu, C. Molnar, A. S. Vasilevich, J.D. Barry, H.S. Bansal, O. Kraus, M. Wawer, L. Paavolainen, M. D. Herrmann, M. Rohban, J. Hung, H. Hennig, J. Concannon, I. Smith, P. A. Clemons, S. Singh, P. Rees, P. Horvath, R.G. Linington, A.E. Carpenter, Data-analysis strategies for image-based cell profiling, Nat. Methods 14 (9) (2017) 849–863.
[5] K. Smith, F. Piccinini, T. Balassa, K. Koos, T. Danka, H. Azizpour, P. Horvath, Phenotypic image analysis software tools for exploring and understanding big image data from cell-based assays, Cell Syst. 6 (6) (2018) 636–653.
[6] M.J. Cox, S. Jaensch, J. Van de Waeter, L. Cougnaud, D. Seynaeve, S. Benalla, S. J. Koo, I. Van Den Wyngaert, J.-M. Neefs, D. Malkov, M. Bittremieux, M. Steemans, P.J. Peeters, J.K. Wegner, H. Ceulemans, E. Gustin, Y.T. Chong, H. W.H. Göhlmann, Tales of 1,008 small molecules: phenomic profiling through live-cell imaging in a panel of reporter cell lines, Sci. Rep. 10 (1) (2020).
[7] Z.E. Perlman, M.D. Slack, Y. Feng, T.J. Mitchison, L.F. Wu, S.J. Altschuler, Multidimensional drug profiling by automated microscopy, Science 306 (5699) (2004) 1194–1198.
[8] S.M. Gustafsdottir, V. Ljosa, K.L. Sokolnicki, J. Anthony Wilson, D. Walpita, M. M. Kemp, K. Petri Seiler, H.A. Carrel, T.R. Golub, S.L. Schreiber, P.A. Clemons, A. E. Carpenter, A.F. Shamji, M. Mancini, Multiplex cytological profiling assay to measure diverse cellular states, PLoS One 8 (12) (2013) e80999.
[9] S. Biswas, High content analysis across signaling modulation treatments for subcellular target identification reveals heterogeneity in cellular response, Front. Cell Dev. Biol. 8 (2020), 594750.
[10] N. Cerisier, B. Dafniet, A. Badel, O. Taboureau, Linking chemicals, genes and morphological perturbations to diseases, Toxicol. Appl. Pharmacol. 15 (461) (2023), 116407.
[11] S. Kremb, C.R. Voolstra, High-resolution phenotypic profiling of natural products-induced effects on the single-cell level, Sci. Rep. 15 (7) (2017) 44472.
[12] P.D. Caie, R.E. Walls, A. Ingleston-Orme, S. Daya, T. Houslay, R. Eagle, et al., High-content phenotypic profiling of drug response signatures across distinct cancer cells, Mol Cancer Ther. 9 (6) (2010) 1913–1926.
[13] F. Reisen, A. Sauty de Chalon, M. Pfeifer, X. Zhang, D. Gabriel, P. Selzer, Linking phenotypes and modes of action through high-content screen fingerprints, Assay Drug Dev. Technol. 13 (7) (2015) 415–427.
[14] D.W. Young, A. Bender, J. Hoyt, E. McWhinnie, G.-W. Chirn, C.Y. Tao, J. A. Tallarico, M. Labow, J.L. Jenkins, T.J. Mitchison, Y. Feng, Integrating high-content screening and ligand-target prediction to identify mechanism of action, Nat. Chem. Biol. 4 (1) (2008) 59–68.
[15] L. Heinrich, K. Kumbier, L. Li, S.J. Altschuler, L.F. Wu, Selection of optimal cell lines for high-content phenotypic screening, ACS Chem. Biol. 18 (4) (2023) 679–685.
[16] S.J. Warchal, J.C. Dawson, N.O. Carragher, Evaluation of machine learning classifiers to predict compound mechanism of action when transferred across distinct cell lines, SLAS Discov. Adv. Life Sci. R D. 24 (3) (2019) 224–233.
[17] M. Ackermann, A functional perspective on phenotypic heterogeneity in microorganisms, Nat. Rev. Microbiol. 13 (8) (2015) 497–508.

[18] F. Schreiber, S. Littmann, G. Lavik, S. Escrig, A. Meibom, M.M.M. Kuypers, et al., Phenotypic heterogeneity driven by nutrient limitation promotes growth in fluctuating environments, Nat. Microbiol. 1 (6) (2016) 16055.

[19] M. Acar, J.T. Mettetal, A. van Oudenaarden, Stochastic switching as a survival strategy in fluctuating environments, Nat. Genet. 40 (4) (2008) 471–475.

[20] S.L. Spencer, S. Gaudet, J.G. Albeck, J.M. Burke, P.K. Sorger, Non-genetic origins of cell-to-cell variability in TRAIL-induced apoptosis, Nature 459 (7245) (2009) 428–432.

[21] A.A. Cohen, N. Geva-Zatorsky, E. Eden, M. Frenkel-Morgenstern, I. Issaeva, A. Sigal, R. Milo, C. Cohen-Saidon, Y. Liron, Z. Kam, L. Cohen, T. Danon, N. Perzov, U. Alon, Dynamic proteomics of individual cancer cells in response to a drug, Science 322 (5907) (2008) 1511–1516.

[22] F. Stossi, R.D. Dandekar, M.G. Mancini, G. Gu, S.A.W. Fuqua, A. Nardone, et al., Estrogen-induced transcription at individual alleles is independent of receptor level and active conformation but can be modulated by coactivators activity, Nucleic Acids Res. 48 (4) (2020) 1800–1810.

[23] K. Bahar Halpern, S. Tanami, S. Landen, M. Chapal, L. Szlak, A. Hutzler, A. Nizhberg, S. Itzkovitz, Bursty gene expression in the intact mammalian liver, Mol. Cell 58 (1) (2015) 147–156.

[24] N. Battich, T. Stoeger, L. Pelkmans, Control of Transcript Variability in Single Mammalian Cells, Cell 163 (7) (2015) 1596–1610.

[25] R.E.C. Lee, S.R. Walker, K. Savery, D.A. Frank, S. Gaudet, Fold change of nuclear NF-κB determines TNF-induced transcription in single cells, Mol. Cell 53 (6) (2014) 867–879.

[26] S.N. Chandrasekaran, H. Ceulemans, J.D. Boyd, A.E. Carpenter, Image-based profiling for drug discovery: due for a machine-learning upgrade? Nat. Rev. Drug Discov. 20 (2) (2021) 145–159.

[27] M.B. Elowitz, A.J. Levine, E.D. Siggia, P.S. Swain, Stochastic gene expression in a single cell, Science 297 (5584) (2002) 1183–1186.

[28] S. Tay, J.J. Hughey, T.K. Lee, T. Lipniacki, S.R. Quake, M.W. Covert, Single-cell NF-kappaB dynamics reveal digital activation and analogue information processing, Nature 466 (7303) (2010) 267–271.

[29] K.L. Garner, High content imaging for monitoring signalling dynamics in single cells, J. Mol. Endocrinol. 65 (4) (2020) R91–R.

[30] F. Stossi, P.K. Singh, R.M. Mistry, H.L. Johnson, R.D. Dandekar, M.G. Mancini, A. T. Szafran, A.U. Rao, M.A. Mancini, Quality Control for Single Cell Imaging Analytics Using Endocrine Disruptor-Induced Changes in Estrogen Receptor Expression, Environ. Health Perspect. 130 (2) (2022).

[31] A. Gough, A.M. Stern, J. Maier, T. Lezon, T.-Y. Shun, C. Chennubhotla, M. E. Schurdak, S.A. Haney, D.L. Taylor, Biologically Relevant Heterogeneity: Metrics and Practical Insights, SLAS Discov Adv Life Sci R D. 22 (3) (2017) 213–237.

[32] A.H. Gough, N. Chen, T.Y. Shun, T.R. Lezon, R.C. Boltz, C.E. Reese, J. Wagner, L. A. Vernetti, J.R. Grandis, A.V. Lee, A.M. Stern, M.E. Schurdak, D.L. Taylor, R. Paulmurugan, Identifying and quantifying heterogeneity in high content analysis: application of heterogeneity indices to drug discovery, PLoS One 9 (7) (2014) e102678.

[33] K.A. Geiler-Samerotte, C.R. Bauer, S. Li, N. Ziv, D. Gresham, M.L. Siegal, The details in the distributions: why and how to study phenotypic variability, Curr. Opin. Biotechnol. 24 (4) (2013) 752–759.

[34] C.M. Garvey, E. Spiller, D. Lindsay, C.-T. Chiang, N.C. Choi, D.B. Agus, P. Mallick, J. Foo, S.M. Mumenthaler, A high-content image-based method for quantitatively studying context-dependent cell population dynamics, Sci. Rep. 6 (1) (2016).

[35] B. Snijder, R. Sacher, P. Rämö, P. Liberali, K. Mench, N. Wolfrum, L. Burleigh, C. C. Scott, M.H. Verheije, J. Mercer, S. Moese, T. Heger, K. Theusner, A. Jurgeit, D. Lamparter, G. Balistreri, M. Schelhaas, C.A.M. De Haan, V. Marjomäki, T. Hyypiä, P.J.M. Rottier, B. Sodeik, M. Marsh, J. Gruenberg, A. Amara, U. Greber, A. Helenius, L. Pelkmans, Single-cell analysis of population context advances RNAi screening at multiple levels, Mol. Syst. Biol. 8 (1) (2012).

[36] G. Gut, M.D. Herrmann, L. Pelkmans, Multiplexed protein maps link subcellular organization to cellular states, Science 361 (6401) (2018).

[37] M. Mattiazzi Usaj, C.H.L. Yeung, H. Friesen, C. Boone, B.J. Andrews, Single-cell image analysis to explore cell-to-cell heterogeneity in isogenic populations, Cell Syst. 12 (6) (2021) 608–621.

[38] F. Stossi, R.D. Dandekar, H. Johnson, P. Lavere, C.E. Foulds, M.G. Mancini, M. A. Mancini, O. Ziouzenkova, Tributyltin chloride (TBT) induces RXRA down-regulation and lipid accumulation in human liver cells, PLoS One 14 (11) (2019) e0224405.

[39] F. Stossi, R.M. Mistry, P.K. Singh, H.L. Johnson, M.G. Mancini, A.T. Szafran, M. A. Mancini, Single-Cell Distribution Analysis of AR Levels by High-Throughput Microscopy in Cell Models: Application for Testing Endocrine-Disrupting Chemicals, SLAS Discov Adv Life Sci R D. 25 (7) (2020) 684–694.

[40] B.L. Emert, C.J. Cote, E.A. Torre, I.P. Dardani, C.L. Jiang, N. Jain, S.M. Shaffer, A. Raj, Variability within rare cell states enables multiple paths toward drug resistance, Nat. Biotechnol. 39 (7) (2021) 865–876.

[41] V. Roukos, T. Misteli, Deep Imaging: the next frontier in microscopy, Histochem. Cell Biol. 142 (2) (2014) 125–131.

[42] V. Roukos, T.C. Voss, C.K. Schmidt, S. Lee, D. Wangsa, T. Misteli, Spatial dynamics of chromosome translocations in living cells, Science 341 (6146) (2013) 660–664.

[43] B. Burman, T. Misteli, G. Pegoraro, Quantitative detection of rare interphase chromosome breaks and translocations by high-throughput imaging, Genome Biol. 16 (1) (2015) 146.

[44] A. Ferro, T. Mestre, P. Carneiro, I. Sahumbaiev, R. Seruca, J.M. Sanches, Blue intensity matters for cell cycle profiling in fluorescence DAPI-stained images, Lab Investig J Tech Methods Pathol. 97 (5) (2017) 615–625.

[45] Y.E. Pearson, S. Kremb, G.L. Butterfoss, X. Xie, H. Fahs, K.C. Gunsalus, A statistical framework for high-content phenotypic profiling using cellular feature distributions, Commun Biol. 5 (1) (2022) 1409.

[46] A. Gough, T.Y. Shun, D. Lansing Taylor, M. Schurdak, A metric and workflow for quality control in the analysis of heterogeneity in phenotypic profiles and screens, Methods San Diego Calif. 1 (96) (2016) 12–26.

[47] L.H. Loo, H.J. Lin, D.K. Singh, K.M. Lyons, S.J. Altschuler, L.F. Wu, Heterogeneity in the physiological states and pharmacological responses of differentiating 3T3-L1 preadipocytes, J Cell Biol. 187 (3) (2009) 375–384.

[48] D.K. Singh, C.J. Ku, C. Wichaidit, R.J. Steininger, L.F. Wu, S.J. Altschuler, Patterns of basal signaling heterogeneity can distinguish cellular populations with different drug sensitivities, Mol. Syst. Biol. 11 (6) (2010) 369.

[49] L.H. Loo, L.F. Wu, S.J. Altschuler, Image-based multivariate profiling of drug responses from single cells, Nat. Methods 4 (5) (2007) 445–453.

[50] M.D. Slack, E.D. Martinez, L.F. Wu, S.J. Altschuler, Characterizing heterogeneous cellular responses to perturbations, PNAS 105 (49) (2008) 19306–19311.

[51] M.-A. Bray, S. Singh, H. Han, C.T. Davis, B. Borgeson, C. Hartland, M. Kost-Alimova, S.M. Gustafsdottir, C.C. Gibson, A.E. Carpenter, Cell Painting, a high-content image-based assay for morphological profiling using multiplexed fluorescent dyes, Nat. Protoc. 11 (9) (2016) 1757–1774.

[52] M.A. Bray, S.M. Gustafsdottir, M.H. Rohban, S. Singh, V. Ljosa, K.L. Sokolnicki, et al., A dataset of images and morphological profiles of 30 000 small-molecule treatments using the Cell Painting assay, GigaScience. 6 (12) (2017) 1–5.

[53] P. Brodin, T. Christophe, High-content screening in infectious diseases, Curr. Opin. Chem. Biol. 15 (4) (2011) 534–539.

[54] M. Breinig, F.A. Klein, W. Huber, M. Boutros, A chemical-genetic interaction map of small molecules using high-throughput imaging in cancer cells, Mol. Syst. Biol. 11 (12) (2015) 846.

[55] N. Kubben, K.R. Brimacombe, M. Donegan, Z. Li, T. Misteli, A high-content imaging-based screening pipeline for the systematic identification of anti-progeroid compounds, Methods San Diego Calif. 1 (96) (2016) 46–58.

[56] A. Ketley, C.Z. Chen, X. Li, S. Arya, T.E. Robinson, J. Granados-Riveron, et al., High-content screening identifies small molecules that remove nuclear foci, affect MBNL distribution and CELF1 protein levels via a PKC-independent pathway in myotonic dystrophy cell lines, Hum Mol Genet. 23 (6) (2014) 1551–1562.

[57] J.o. Nyffeler, C. Willis, F.R. Harris, M.J. Foster, B. Chambers, M. Culbreth, R. E. Brockway, S. Davidson-Fritz, D. Dawson, I. Shah, K.P. Friedman, D. Chang, L. J. Everett, J.F. Wambaugh, G. Patlewicz, J.A. Harrill, Application of Cell Painting for chemical hazard evaluation in support of screening-level chemical assessments, Toxicol. Appl. Pharmacol. 468 (2023) 116513.

[58] J. Nyffeler, C. Willis, R. Lougee, A. Richard, K. Paul-Friedman, J.A. Harrill, Bioactivity screening of environmental chemicals using imaging-based high-throughput phenotypic profiling, Toxicol. Appl. Pharmacol. 15 (389) (2020), 114876.

[59] C. Willis, J. Nyffeler, J. Harrill, Phenotypic Profiling of Reference Chemicals across Biologically Diverse Cell Types Using the Cell Painting Assay, SLAS Discov Adv Life Sci R D. 25 (7) (2020) 755–769.

[60] C.J. Gerry, B.K. Hua, M.J. Wawer, J.P. Knowles, S.D. Nelson Jr., O. Verho, S. Dandapani, B.K. Wagner, P.A. Clemons, K.I. Booker-Milburn, Z.V. Boskovic, S. L. Schreiber, Real-Time Biological Annotation of Synthetic Compounds, J. Am. Chem. Soc. 138 (28) (2016) 8920–8927.

[61] M.J. Wawer, K. Li, S.M. Gustafsdottir, V. Ljosa, N.E. Bodycombe, M.A. Marton, K. L. Sokolnicki, M.-A. Bray, M.M. Kemp, E. Winchester, B. Taylor, G.B. Grant, C.-Y. Hon, J.R. Duvall, J.A. Wilson, J.A. Bittker, V. Dančík, R. Narayan, A. Subramanian, W. Winckler, T.R. Golub, A.E. Carpenter, A.F. Shamji, S. L. Schreiber, P.A. Clemons, Toward performance-diverse small-molecule libraries for cell-based phenotypic screening using multiplexed high-dimensional profiling, PNAS 111 (30) (2014) 10911–10916.

[62] M.-A. Trapotsi, E. Mouchet, G. Williams, T. Monteverde, K. Juhani, R. Turkki, F. Miljković, A. Martinsson, L. Mervin, K.R. Pryde, E. Müllers, I. Barrett, O. Engkvist, A. Bender, K. Moreau, Cell Morphological Profiling Enables High-Throughput Screening for PROteolysis TArgeting Chimera (PROTAC) Phenotypic Signature, ACS Chem. Biol. 17 (7) (2022) 1733–1744.

[63] G. Pegoraro, T. Misteli, High-Throughput Imaging for the Discovery of Cellular Mechanisms of Disease, Trends Genet TIG. 33 (9) (2017) 604–615.

[64] A.K. Glaser, N.P. Reder, Y.e. Chen, C. Yin, L. Wei, S. Kang, L.A. Barner, W. Xie, E. F. McCarty, C. Mao, A.R. Halpern, C.R. Stoltzfus, J.S. Daniels, M.Y. Gerner, P. R. Nicovich, J.C. Vaughan, L.D. True, J.T.C. Liu, Multi-immersion open-top light-sheet microscope for high-throughput imaging of cleared tissues, Nat. Commun. 10 (1) (2019).

[65] M. Bernardello, E.J. Gualda, P. Loza-Alvarez, Modular multimodal platform for classical and high throughput light sheet microscopy, Sci. Rep. 12 (1) (2022) 1969.

[66] J.L. Dahlin, B.K. Hua, B.E. Zucconi, S.D. Nelson, S. Singh, A.E. Carpenter, J. H. Shrimp, E. Lima-Fernandes, M.J. Wawer, L.P.W. Chung, A. Agrawal, M. O'Reilly, D. Barsyte-Lovejoy, M. Szewczyk, F. Li, P. Lak, M. Cuellar, P.A. Cole, J.L. Meier, T. Thomas, J.B. Baell, P.J. Brown, M.A. Walters, P.A. Clemons, S. L. Schreiber, B.K. Wagner, Reference compounds for characterizing cellular injury in high-content cellular morphology assays, Nat. Commun. 14 (1) (2023).

[67] G.P. Way, M. Kost-Alimova, T. Shibue, W.F. Harrington, S. Gill, F. Piccioni, T. Becker, H. Shafqat-Abbasi, W.C. Hahn, A.E. Carpenter, F. Vazquez, S. Singh, A. Mogilner, Predicting cell health phenotypes using image-based morphology profiling, Mol. Biol. Cell 32 (9) (2021) 995–1005.

[68] E. Finn, T. Misteli, G. Pegoraro, High-Throughput DNA FISH (hiFISH), Methods Mol Biol Clifton NJ. 2532 (2022) 245–274.

[69] M. Skogs, C. Stadler, R. Schutten, M. Hjelmare, C. Gnann, L. Björk, I. Poser, A. Hyman, M. Uhlén, E. Lundberg, Antibody Validation in Bioimaging Applications Based on Endogenous Expression of Tagged Proteins, J. Proteome Res. 16 (1) (2017) 147–155.

[70] C. Stadler, M. Hjelmare, B. Neumann, K. Jonasson, R. Pepperkok, M. Uhlén, E. Lundberg, Systematic validation of antibody binding and protein subcellular localization using siRNA and confocal microscopy, J. Proteomics 75 (7) (2012) 2236–2251.

[71] C. Stadler, E. Rexhepaj, V.R. Singan, R.F. Murphy, R. Pepperkok, M. Uhlén, J. C. Simpson, E. Lundberg, Immunofluorescence and fluorescent-protein tagging show high correlation for protein localization in mammalian cells, Nat. Methods 10 (4) (2013) 315–323.

[72] R.M. Mistry, P.K. Singh, M.G. Mancini, F. Stossi, M.A. Mancini, Single Cell Analysis Of Transcriptionally Active Alleles By Single Molecule FISH, Journal of Visualized ExperimentsJoVE. (2020;(163).).

[73] Sexton JZ, Fursmidt R, O'Meara MJ, Omta W, Rao A, Egan DA, et al. Machine Learning and Assay Development for Image-based Phenotypic Profiling of Drug Treatments. In: Markossian S, Grossman A, Brimacombe K, Arkin M, Auld D, Austin C, et al., editors. Assay Guidance Manual [Internet]. Bethesda (MD): Eli Lilly & Company and the National Center for Advancing Translational Sciences; 2004 [cited 2023 May 18]. Available from: http://www.ncbi.nlm.nih.gov/books/NBK589577/.

[74] N. Malo, J.A. Hanley, S. Cerquozzi, J. Pelletier, R. Nadon, Statistical practice in high-throughput screening data analysis, Nat. Biotechnol. 24 (2) (2006) 167–175.

[75] S. Markossian, K.R. Brimacombe, G.S. Sittampalam, A. Grossman, N.P. Coussens, J. Inglese, D.S. Auld, W. Chin, C.P. Austin, M.D. Hall, The NCATS Assay Guidance Manual programme: advancing the practice and rigour of preclinical translation, Nat. Rev. Drug Discov. 21 (12) (2022) 863–864.

[76] V. Blay, B. Tolani, S.P. Ho, M.R. Arkin, High-Throughput Screening: today's biochemical and cell-based approaches, Drug Discov. Today 25 (10) (2020) 1807–1821.

[77] S. Lin, K. Schorpp, I. Rothenaigner, K. Hadian, Image-based high-content screening in drug discovery, Drug Discov. Today 25 (8) (2020) 1348–1361.

[78] B.T. Grys, D.S. Lo, N. Sahin, O.Z. Kraus, Q. Morris, C. Boone, et al., Machine learning and computer vision approaches for phenotypic profiling, J Cell Biol. 216 (1) (2017) 65–71.

[79] O.Z. Kraus, B.T. Grys, J. Ba, Y. Chong, B.J. Frey, C. Boone, et al., Automated analysis of high-content microscopy data with deep learning, Mol. Syst. Biol. 13 (4) (2017) 924.

[80] A. Pratapa, M. Doron, J.C. Caicedo, Image-based cell phenotyping with deep learning, Curr. Opin. Chem. Biol. 65 (2021) 9–17.

[81] F. Garcia-Fossa, M.C. Cruz, M. Haghighi, M.B. de Jesus, S. Singh, A.E. Carpenter, B.A. Cimini, Interpreting Image-based Profiles using Similarity Clustering and Single-Cell Visualization, Curr Protoc. 3 (3) (2023) e713.

[82] T. Wollmann, H. Erfle, R. Eils, K. Rohr, M. Gunkel, Workflows for microscopy image analysis and cellular phenotyping, J. Biotechnol. 10 (261) (2017) 70–75.

[83] K.A. Giuliano, D.L. Taylor, Fluorescent-protein biosensors: new tools for drug discovery, Trends Biotechnol. 16 (3) (1998) 135–140.

[84] S. Singh, M.A. Bray, T.R. Jones, A.E. Carpenter, Pipeline for illumination correction of images for high-throughput microscopy, J. Microsc. 256 (3) (2014) 231–236.

[85] M. Pachitariu, C. Stringer, Cellpose 2.0: how to train your own model, Nat. Methods 19 (12) (2022) 1634–1641.

[86] J.J.M. van Griethuysen, A. Fedorov, C. Parmar, A. Hosny, N. Aucoin, V. Narayan, et al., Computational radiomics system to decode the radiographic phenotype, Cancer Res. 77 (21) (2017) e104–7.

[87] S. van der Walt, J.L. Schönberger, J. Nunez-Iglesias, F. Boulogne, J.D. Warner, N. Yager, E. Gouillart, T. Yu, scikit-image: image processing in Python, PeerJ 2 (2014) e453.

[88] C. McQuin, A. Goodman, V. Chernyshev, L. Kamentsky, B.A. Cimini, K. W. Karhohs, M. Doan, L. Ding, S.M. Rafelski, D. Thirstrup, W. Wiegraebe, S. Singh, T. Becker, J.C. Caicedo, A.E. Carpenter, T. Misteli, Cell Profiler 3.0: Next-generation image processing for biology, PLoS Biol. 16 (7) (2018) e2005970.

[89] N. Jamali, C. Tromans-Coia, H.S. Abbasi, K.A. Giuliano, M. Hagimoto, K. Jan, et al., Assessing the performance of the Cell Painting assay across different imaging systems, BioRxiv Prepr Serv Biol. (2023), 2023.02.15.528711.

[90] A. Kensert, P.J. Harrison, O. Spjuth, Transfer learning with deep convolutional neural networks for classifying cellular morphological changes, SLAS Discov Adv Life Sci R D. 24 (4) (2019) 466–475.

[91] C. Scheeder, F. Heigwer, M. Boutros, Machine learning and image-based profiling in drug discovery, Curr Opin Syst Biol. 10 (2018) 43–52.

[92] V. Ljosa, P.D. Caie, R. ter Horst, K.L. Sokolnicki, E.L. Jenkins, S. Daya, M. E. Roberts, T.R. Jones, S. Singh, A. Genovesio, P.A. Clemons, N.O. Carragher, A. E. Carpenter, Comparison of methods for image-based profiling of cellular morphological responses to small-molecule treatment, J. Biomol. Screen. 18 (10) (2013) 1321–1329.

[93] S.J. Warchal, J.C. Dawson, N.O. Carragher, High-Dimensional Profiling: The Theta Comparative Cell Scoring Method, Methods Mol Biol Clifton NJ. 1787 (2018) 171–181.

[94] S.J. Warchal, J.C. Dawson, N.O. Carragher, Development of the Theta Comparative Cell Scoring Method to Quantify Diverse Phenotypic Responses Between Distinct Cell Types, Assay Drug Dev. Technol. 14 (7) (2016) 395–406.

[95] S.J. Haggarty, T.U. Mayer, D.T. Miyamoto, R. Fathi, R.W. King, T.J. Mitchison, S. L. Schreiber, Dissecting cellular processes using small molecules: identification of colchicine-like, taxol-like and other small molecules that perturb mitosis, Chem. Biol. 7 (4) (2000) 275–286.

[96] D.L.C. Almholt, F. Loechel, S.J. Nielsen, C. Krog-Jensen, R. Terry, S.P. Bjørn, H. C. Pedersen, M. Praestegaard, S. Møller, M. Heide, L. Pagliaro, A.J. Mason, S. Butcher, S.W. Dahl, Nuclear export inhibitors and kinase inhibitors identified using a MAPK-activated protein kinase 2 redistribution screen, Assay Drug Dev. Technol. 2 (1) (2004) 7–20.

[97] A. Vogt, K.A. Cooley, M. Brisson, M.G. Tarpley, P. Wipf, J.S. Lazo, Cell-active dual specificity phosphatase inhibitors identified by high-content screening, Drug Discov. Today (2005). Suppl:3–12.

[98] K.R. Atanasova, S. Chakraborty, R. Ratnayake, K.D. Khare, H. Luesch, T.P. Lele, J. Lippincott-Schwartz, An epigenetic small molecule screen to target abnormal nuclear morphology in human cells, Mol. Biol. Cell 33 (6) (2022).

[99] A. Corman, D.C. Kanellis, P. Michalska, M. Häggblad, V. Lafarga, J. Bartek, et al., A chemical screen for modulators of mRNA translation identifies a distinct mechanism of toxicity for sphingosine kinase inhibitors, PLoS Biol. 19 (5) (2021).

[100] M. Gendarme, J. Baumann, T.I. Ignashkova, R.K. Lindemann, J.H. Reiling, A. Nakano, Image-based drug screen identifies HDAC inhibitors as novel Golgi disruptors synergizing with JQ1, Mol. Biol. Cell 28 (26) (2017) 3756–3772.

[101] S.K. Hight, T.N. Clark, K.L. Kurita, E.A. McMillan, W. Bray, A.F. Shaikh, et al., High-throughput functional annotation of natural products by integrated activity profiling, Proc Natl Acad Sci U S A. 119 (49) (2022).

[102] J. Barretina, G. Caponigro, N. Stransky, K. Venkatesan, A.A. Margolin, S. Kim, et al., The Cancer Cell Line Encyclopedia enables predictive modelling of anticancer drug sensitivity, Nature 483 (7391) (2012) 603–607.

[103] M.J. Garnett, E.J. Edelman, S.J. Heidorn, C.D. Greenman, A. Dastur, K.W. Lau, P. Greninger, I.R. Thompson, X.i. Luo, J. Soares, Q. Liu, F. Iorio, D. Surdez, L. i. Chen, R.J. Milano, G.R. Bignell, A.T. Tam, H. Davies, J.A. Stevenson, S. Barthorpe, S.R. Lutz, F. Kogera, K. Lawrence, A. McLaren-Douglas, X. Mitropoulos, T. Mironenko, H. Thi, L. Richardson, W. Zhou, F. Jewitt, T. Zhang, P. O'Brien, J.L. Boisvert, S. Price, W. Hur, W. Yang, X. Deng, A. Butler, H.G. Choi, J.W. Chang, J. Baselga, I. Stamenkovic, J.A. Engelman, S.V. Sharma, O. Delattre, J. Saez-Rodriguez, N.S. Gray, J. Settleman, P.A. Futreal, D.A. Haber, M. R. Stratton, S. Ramaswamy, U. McDermott, C.H. Benes, Systematic identification of genomic markers of drug sensitivity in cancer cells, Nature 483 (7391) (2012) 570–575.

[104] C.J. Torrance, V. Agrawal, B. Vogelstein, K.W. Kinzler, Use of isogenic human cancer cells for high-throughput screening and drug discovery, Nat. Biotechnol. 19 (10) (2001) 940–945.

[105] M.K. Muellner, I.Z. Uras, B.V. Gapp, C. Kerzendorfer, M. Smida, H. Lechtermann, N. Craig-Mueller, J. Colinge, G. Duernberger, S.M.B. Nijman, A chemical-genetic screen reveals a mechanism of resistance to PI3K inhibitors in cancer, Nat. Chem. Biol. 7 (11) (2011) 787–793.

[106] S. Kittanakom, A. Arnoldo, K.R. Brown, I. Wallace, T. Kunavisarut, D. Torti, et al., Miniature short hairpin RNA screens to characterize antiproliferative drugs, G3 Bethesda Md. 3 (8) (2013) 1375–1387.

[107] A. Tjaden, A. Chaikuad, E. Kowarz, R. Marschalek, S. Knapp, M. Schröder, S. Müller, Image-Based Annotation of Chemogenomic Libraries for Phenotypic Screening, Mol Basel Switz. 27 (4) (2022) 1439.

[108] F. Wippich, B. Bodenmiller, M.G. Trajkovska, S. Wanka, R. Aebersold, L. Pelkmans, Dual specificity kinase DYRK3 couples stress granule condensation/dissolution to mTORC1 signaling, Cell 152 (4) (2013) 791–805.

[109] L.M. Ogawa, A.F. Buhagiar, L. Abriola, B.A. Leland, Y.V. Surovtseva, S.J. Baserga, J. Lippincott-Schwartz, Increased numbers of nucleoli in a genome-wide RNAi screen reveal proteins that link the cell cycle to RNA polymerase I transcription, Mol. Biol. Cell 32 (9) (2021) 956–973.

[110] S. Hussain, X. Le Guezennec, W. Yi, H. Dong, J. Chia, K.e. Yiping, L.K. Khoon, F. Bard, T. Sommer, Digging deep into Golgi phenotypic diversity with unsupervised machine learning, Mol. Biol. Cell 28 (25) (2017) 3686–3698.

[111] B. Neumann, M. Held, U. Liebel, H. Erfle, P. Rogers, R. Pepperkok, J. Ellenberg, High-throughput RNAi screening by time-lapse imaging of live human cells, Nat. Methods 3 (5) (2006) 385–390.

[112] B. Neumann, T. Walter, J.-K. Hériché, J. Bulkescher, H. Erfle, C. Conrad, P. Rogers, I. Poser, M. Held, U. Liebel, C. Cetin, F. Sieckmann, G. Pau, R. Kabbe, A. Wünsche, V. Satagopam, M.H.A. Schmitz, C. Chapuis, D.W. Gerlich, R. Schneider, R. Eils, W. Huber, J.-M. Peters, A.A. Hyman, R. Durbin, R. Pepperkok, J. Ellenberg, Phenotypic profiling of the human genome by time-lapse microscopy reveals cell division genes, Nature 464 (7289) (2010) 721–727.

[113] M.H.A. Schmitz, M. Held, V. Janssens, J.R.A. Hutchins, O. Hudecz, E. Ivanova, et al., Live-cell imaging RNAi screen identifies PP2A-B55alpha and importin-beta1 as key mitotic exit regulators in human cells, Nat. Cell Biol. 12 (9) (2010) 886–893.

[114] L. Pelkmans, E. Fava, H. Grabner, M. Hannus, B. Habermann, E. Krausz, M. Zerial, Genome-wide analysis of human kinases in clathrin- and caveolae/raft-mediated endocytosis, Nature 436 (7047) (2005) 78–86.

[115] C. Collinet, M. Stöter, C.R. Bradshaw, N. Samusik, J.C. Rink, D. Kenski, B. Habermann, F. Buchholz, R. Henschel, M.S. Mueller, W.E. Nagel, E. Fava, Y. Kalaidzidis, M. Zerial, Systems survey of endocytosis by multiparametric image analysis, Nature 464 (7286) (2010) 243–249.

[116] P. Liberali, B. Snijder, L. Pelkmans, A hierarchical map of regulatory genetic interactions in membrane trafficking, Cell 157 (6) (2014) 1473–1487.

[117] B. Adamson, A. Smogorzewska, F.D. Sigoillot, R.W. King, S.J. Elledge, A genome-wide homologous recombination screen identifies the RNA-binding protein RBMX as a component of the DNA-damage response, Nat. Cell Biol. 14 (3) (2012) 318–328.

[118] B.C. O'Connell, B. Adamson, J.R. Lydeard, M.E. Sowa, A. Ciccia, A.L. Bredemeyer, M. Schlabach, S.P. Gygi, S.J. Elledge, J.W. Harper, A genome-wide camptothecin sensitivity screen identifies a mammalian MMS22L-NFKBIL2 complex required for genomic stability, Mol. Cell 40 (4) (2010) 645–657.
[119] A. Orvedahl, R. Sumpter, G. Xiao, A. Ng, Z. Zou, Y.i. Tang, M. Narimatsu, C. Gilpin, Q. Sun, M. Roth, C.V. Forst, J.L. Wrana, Y.E. Zhang, K. Luby-Phelps, R. J. Xavier, Y. Xie, B. Levine, Image-based genome-wide siRNA screen identifies selective autophagy factors, Nature 480 (7375) (2011) 113–117.
[120] S.A. Hasson, L.A. Kane, K. Yamano, C.-H. Huang, D.A. Sliter, E. Buehler, C. Wang, S.M. Heman-Ackah, T. Hessa, R. Guha, S.E. Martin, R.J. Youle, High-content genome-wide RNAi screens identify regulators of parkin upstream of mitophagy, Nature 504 (7479) (2013) 291–295.
[121] F. Fuchs, G. Pau, D. Kranz, O. Sklyar, C. Budjan, S. Steinbrink, T. Horn, A. Pedal, W. Huber, M. Boutros, Clustering phenotype populations by genome-wide RNAi and multiparametric imaging, Mol. Syst. Biol. 6 (1) (2010).
[122] S. Shachar, T.C. Voss, G. Pegoraro, N. Sciascia, T. Misteli, Identification of Gene Positioning Factors Using High-Throughput Imaging Mapping, Cell 162 (4) (2015) 911–923.
[123] J. Tan, S.E. Martin, H. Fujii, Validation of Synthetic CRISPR Reagents as a Tool for Arrayed Functional Genomic Screening, PLoS One 11 (12) (2016) e0168968.
[124] X. Yan, N. Stuurman, S.A. Ribeiro, M.E. Tanenbaum, M.A. Horlbeck, C.R. Liem, et al., High-content imaging-based pooled CRISPR screens in mammalian cells, J Cell Biol. 220 (2) (2021).
[125] M. Lawson, J. Elf, Imaging-based screens of pool-synthesized cell libraries, Nat. Methods 18 (4) (2021) 358–365.
[126] G. Kanfer, S.A. Sarraf, Y. Maman, H. Baldwin, E. Dominguez-Martin, K. R. Johnson, et al., Image-based pooled whole-genome CRISPRi screening for subcellular phenotypes, J Cell Biol. 220 (2) (2021).
[127] R.T. Walton, A. Singh, P.C. Blainey, Pooled genetic screens with image-based profiling, Mol. Syst. Biol. 18 (11) (2022) e10768.
[128] R. de Groot, J. Lüthi, H. Lindsay, R. Holtackers, L. Pelkmans, Large-scale image-based profiling of single-cell phenotypes in arrayed CRISPR-Cas9 gene perturbation screens, Mol. Syst. Biol. 14 (1) (2018) e8064.
[129] D. Feldman, A. Singh, J.L. Schmid-Burgk, R.J. Carlson, A. Mezger, A.J. Garrity, F. Zhang, P.C. Blainey, Optical Pooled Screens in Human Cells, Cell 179 (3) (2019) 787–799.e17.
[130] D. Feldman, L. Funk, A. Le, R.J. Carlson, M.D. Leiken, FuNien Tsai, B. Soong, A. Singh, P.C. Blainey, Pooled genetic perturbation screens with image-based phenotypes, Nat. Protoc. 17 (2) (2022) 476–512.
[131] E.C. Wheeler, A.Q. Vu, J.M. Einstein, M. DiSalvo, N. Ahmed, E.L. Van Nostrand, A.A. Shishkin, W. Jin, N.L. Allbritton, G.W. Yeo, Pooled CRISPR screens with imaging on microraft arrays reveals stress granule-regulatory factors, Nat. Methods 17 (6) (2020) 636–642.
[132] N. Hasle, A. Cooke, S. Srivatsan, H. Huang, J.J. Stephany, Z. Krieger, D. Jackson, W. Tang, S. Pendyala, R.J. Monnat, C. Trapnell, E.M. Hatch, D.M. Fowler, High-throughput, microscope-based sorting to dissect cellular heterogeneity, Mol. Syst. Biol. 16 (6) (2020) e9442.
[133] L. Funk, K.-C. Su, J. Ly, D. Feldman, A. Singh, B. Moodie, P.C. Blainey, I. M. Cheeseman, The phenotypic landscape of essential human genes, Cell 185 (24) (2022) 4634–4653.e22.
[134] C. Wang, T. Lu, G. Emanuel, H.P. Babcock, X. Zhuang, Imaging-based pooled CRISPR screening reveals regulators of lncRNA localization, PNAS 116 (22) (2019) 10842–10851.
[135] M.J. Wawer, D.E. Jaramillo, V. Dančík, D.M. Fass, S.J. Haggarty, A.F. Shamji, B. K. Wagner, S.L. Schreiber, P.A. Clemons, Automated Structure-Activity Relationship Mining: Connecting Chemical Structure to Biological Profiles, J. Biomol. Screen. 19 (5) (2014) 738–748.
[136] M.H. Rohban, S. Singh, X. Wu, J.B. Berthet, M.-A. Bray, Y. Shrestha, X. Varelas, J. S. Boehm, A.E. Carpenter, Systematic morphological profiling of human gene and allele function via Cell Painting, Elife 6 (2017) e24060.
[137] J.C. Caicedo, C. McQuin, A. Goodman, S. Singh, A.E. Carpenter, Weakly Supervised Learning of Single-Cell Feature Embeddings, Proc IEEE Comput Soc Conf Comput Vis Pattern Recognit. 2018 (2018) 9309–9318.
[138] A. Christoforow, J. Wilke, A. Binici, A. Pahl, C. Ostermann, S. Sievers, H. Waldmann, Design, Synthesis, and Phenotypic Profiling of Pyrano-Furo-Pyridone Pseudo Natural Products, Angew. Chem. Int. Ed. Engl. 58 (41) (2019) 14715–14723.
[139] A. Pahl, S. Sievers, The Cell Painting Assay as a Screening Tool for the Discovery of Bioactivities in New Chemical Matter, Methods Mol Biol Clifton NJ. 1888 (2019) 115–126.
[140] R.E. Hughes, R.J.R. Elliott, A.F. Munro, A. Makda, J.R. O'Neill, T. Hupp, N. O. Carragher, High-Content Phenotypic Profiling in Esophageal Adenocarcinoma Identifies Selectively Active Pharmacological Classes of Drugs for Repurposing and Chemical Starting Points for Novel Drug Discovery, SLAS Discov Adv Life Sci R D. 25 (7) (2020) 770–782.
[141] J.L. Ochoa, W.M. Bray, R.S. Lokey, R.G. Linington, Phenotype-Guided Natural Products Discovery Using Cytological Profiling, J. Nat. Prod. 78 (9) (2015) 2242–2248.
[142] G.P. Way, T. Natoli, A. Adeboye, L. Litichevskiy, A. Yang, X. Lu, J.C. Caicedo, B. A. Cimini, K. Karhohs, D.J. Logan, M.H. Rohban, M. Kost-Alimova, K. Hartland, M. Bornholdt, S.N. Chandrasekaran, M. Haghighi, E. Weisbart, S. Singh, A. Subramanian, A.E. Carpenter, Morphology and gene expression profiling provide complementary information for mapping cell state, Cell Syst. 13 (11) (2022) 911–923.e9.
[143] A. Howarth, M. Schröder, R.C. Montenegro, D.H. Drewry, H. Sailem, V. Millar, S. Müller, D.V. Ebner, HighVia-A flexible live-cell high-content screening pipeline to assess cellular toxicity, SLAS Discov Adv Life Sci R D. 25 (7) (2020) 801–811.
[144] A. Safieddine, E. Coleno, F. Lionneton, A.-M. Traboulsi, S. Salloum, C.-H. Lecellier, T. Gostan, V. Georget, C. Hassen-Khodja, A. Imbert, F. Mueller, T. Walter, M. Peter, E. Bertrand, HT-smFISH: a cost-effective and flexible workflow for high-throughput single-molecule RNA imaging, Nat. Protoc. 18 (1) (2023) 157–187.
[145] A. Shilo, G. Pegoraro, T. Misteli, HiFENS: high-throughput FISH detection of endogenous pre-mRNA splicing isoforms, Nucleic Acids Res. 50 (22) (2022).
[146] I. Lukonin, M. Zinner, P. Liberali, Organoids in image-based phenotypic chemical screens, Exp. Mol. Med. 53 (10) (2021) 1495–1502.
[147] S. Hou, H. Tiriac, B.P. Sridharan, L. Scampavia, F. Madoux, J. Seldin, G.R. Souza, D. Watson, D. Tuveson, T.P. Spicer, Advanced Development of Primary Pancreatic Organoid Tumor Models for High-Throughput Phenotypic Drug Screening, SLAS Discov Adv Life Sci R D. 23 (6) (2018) 574–584.
[148] K. Boehnke, P.W. Iversen, D. Schumacher, M.J. Lallena, R. Haro, J. Amat, J. Haybaeck, S. Liebs, M. Lange, R. Schäfer, C.R.A. Regenbrecht, C. Reinhard, J. A. Velasco, Assay Establishment and Validation of a High-Throughput Screening Platform for Three-Dimensional Patient-Derived Colon Cancer Organoid Cultures, J. Biomol. Screen. 21 (9) (2016) 931–941.
[149] S. Kim, S. Choung, R.X. Sun, N. Ung, N. Hashemi, E.J. Fong, R. Lau, E. Spiller, J. Gasho, J. Foo, S.M. Mumenthaler, Comparison of Cell and Organoid-Level Analysis of Patient-Derived 3D Organoids to Evaluate Tumor Cell Growth Dynamics and Drug Response, SLAS Discov Adv Life Sci R D. 25 (7) (2020) 744–754.
[150] N. Choo, S. Ramm, J. Luu, J.M. Winter, L.A. Selth, A.R. Dwyer, M. Frydenberg, J. Grummet, S. Sandhu, T.E. Hickey, W.D. Tilley, R.A. Taylor, G.P. Risbridger, M. G. Lawrence, K.J. Simpson, High-Throughput Imaging Assay for Drug Screening of 3D Prostate Cancer Organoids, SLAS Discov Adv Life Sci R D. 26 (9) (2021) 1107–1124.
[151] F. Pampaloni, E.G. Reynaud, E.H.K. Stelzer, The third dimension bridges the gap between cell culture and live tissue, Nat. Rev. Mol. Cell Biol. 8 (10) (2007) 839–845.
[152] S.A. Langhans, Three-Dimensional in Vitro Cell Culture Models in Drug Discovery and Drug Repositioning, Front. Pharmacol. 9 (2018) 6.
[153] M. Ravi, V. Paramesh, S.R. Kaviya, E. Anuradha, F.D.P. Solomon, 3D cell culture systems: advantages and applications, J. Cell. Physiol. 230 (1) (2015) 16–26.
[154] R. Edmondson, J.J. Broglie, A.F. Adcock, L. Yang, Three-dimensional cell culture systems and their applications in drug discovery and cell-based biosensors, Assay Drug Dev. Technol. 12 (4) (2014) 207–218.
[155] S.-L. Ryan, A.-M. Baird, G. Vaz, A.J. Urquhart, H. Senge, D.J. Richard, K. J. O'Byrne, A.M. Davies, Drug Discovery Approaches Utilizing Three-Dimensional Cell Culture, Assay Drug Dev. Technol. 14 (1) (2016) 19–28.
[156] K. Stock, M.F. Estrada, S. Vidic, K. Gjerde, A. Rudisch, V.E. Santo, M. Barbier, S. Blom, S.C. Arundkar, I. Selvam, A. Osswald, Y. Stein, S. Gruenewald, C. Brito, W. van Weerden, V. Rotter, E. Boghaert, M. Oren, W. Sommergruber, Y. Chong, R. de Hoogt, R. Graeser, Capturing tumor complexity in vitro: Comparative analysis of 2D and 3D tumor models for drug discovery, Sci. Rep. 6 (1) (2016).
[157] M. Zanoni, F. Piccinini, C. Arienti, A. Zamagni, S. Santi, R. Polico, A. Bevilacqua, A. Tesei, 3D tumor spheroid models for in vitro therapeutic screening: a systematic approach to enhance the biological relevance of data obtained, Sci. Rep. 6 (1) (2016).
[158] S. Sebens, H. Schafer, The tumor stroma as mediator of drug resistance–a potential target to improve cancer therapy? Curr. Pharm. Biotechnol. 13 (11) (2012) 2259–2272.
[159] C. Bonnans, J. Chou, Z. Werb, Remodelling the extracellular matrix in development and disease, Nat. Rev. Mol. Cell Biol. 15 (12) (2014) 786–801.
[160] T. Muranen, L. Selfors, D. Worster, M. Iwanicki, L. Song, F. Morales, S. Gao, G. Mills, J. Brugge, Inhibition of PI3K/mTOR leads to adaptive resistance in matrix-attached cancer cells, Cancer Cell 21 (2) (2012) 227–239.
[161] A.W. Holle, J.L. Young, J.P. Spatz, In vitro cancer cell-ECM interactions inform in vivo cancer treatment, Adv. Drug Deliv. Rev. 1 (97) (2016) 270–279.
[162] F. Bordeleau, B.N. Mason, E.M. Lollis, M. Mazzola, M.R. Zanotelli, S. Somasegar, J.P. Califano, C. Montague, D.J. LaValley, J. Huynh, N. Mencia-Trinchant, Y. L. Negrón Abril, D.C. Hassane, L.J. Bonassar, J.T. Butcher, R.S. Weiss, C. A. Reinhart-King, Matrix stiffening promotes a tumor vasculature phenotype, PNAS 114 (3) (2017) 492–497.
[163] C.H. Lin, T. Jokela, J. Gray, M.A. LaBarge, Combinatorial Microenvironments Impose a Continuum of Cellular Responses to a Single Pathway-Targeted Anti-cancer Compound, Cell Rep. 21 (2) (2017) 533–545.
[164] S.M. Badr-Eldin, H.M. Aldawsari, S. Kotta, P.K. Deb, K.N. Venugopala, Three-Dimensional In Vitro Cell Culture Models for Efficient Drug Discovery: Progress So Far and Future Prospects, Pharm Basel Switz. 15 (8) (2022) 926.
[165] P. Baillargeon, V. Fernandez-Vega, L. Ortiz, J. Shumate, N. Marques, L. Deng, T. P. Spicer, L. Scampavia, Rapid deployment of inexpensive open-source orbital shakers in support of high-throughput screening, SLAS Technol. 27 (3) (2022) 180–186.
[166] D.M. Timm, J. Chen, D. Sing, J.A. Gage, W.L. Haisler, S.K. Neeley, R.M. Raphael, M. Dehghani, K.P. Rosenblatt, T.C. Killian, H. Tseng, G.R. Souza, A high-throughput three-dimensional cell migration assay for toxicity screening with mobile device-based macroscopic image analysis, Sci. Rep. 3 (1) (2013).
[167] T.J. Puls, X. Tan, M. Husain, C.F. Whittington, M.L. Fishel, S.L. Voytik-Harbin, Development of a Novel 3D Tumor-tissue Invasion Model for High-throughput, High-content Phenotypic Drug Screening, Sci. Rep. 8 (1) (2018) 13039.

[168] T.H. Booij, L.S. Price, E.H.J. Danen, 3D Cell-Based Assays for Drug Screens: Challenges in Imaging, Image Analysis, and High-Content Analysis, SLAS Discov Adv Life Sci R D. 24 (6) (2019) 615–627.
[169] M.E. Boutin, T.C. Voss, S.A. Titus, K. Cruz-Gutierrez, S. Michael, M. Ferrer, A high-throughput imaging and nuclear segmentation analysis protocol for cleared 3D culture models, Sci. Rep. 8 (1) (2018) 11135.
[170] T. Zhu, J. Nie, T. Yu, D. Zhu, Y. Huang, Z. Chen, et al., Large-scale high-throughput 3D culture, imaging, and analysis of cell spheroids using microchip-enhanced light-sheet microscopy, Biomed Opt Express. 14 (4) (2023) 1659–1669.
[171] N.a. Zhao, R.T. Powell, X. Yuan, G. Bae, K.P. Roarty, F. Stossi, M. Strempfl, M. J. Toneff, H.L. Johnson, S.A. Mani, P. Jones, C.C. Stephan, J.M. Rosen, Morphological screening of mesenchymal mammary tumor organoids to identify drugs that reverse epithelial-mesenchymal transition, Nat. Commun. 12 (1) (2021).
[172] J.P. Celli, I. Rizvi, A.R. Blanden, I. Massodi, M.D. Glidden, B.W. Pogue, et al., An imaging-based platform for high-content, quantitative evaluation of therapeutic response in 3D tumour models, Sci. Rep. 17 (4) (2014) 3751.
[173] J. Betge, N. Rindtorff, J. Sauer, B. Rauscher, C. Dingert, H. Gaitantzi, F. Herweck, K. Srour-Mhanna, T. Miersch, E. Valentini, K.E. Boonekamp, V. Hauber, T. Gutting, L. Frank, S. Belle, T. Gaiser, I. Buchholz, R. Jesenofsky, N. Härtel, T. Zhan, B. Fischer, K. Breitkopf-Heinlein, E. Burgermeister, M.P. Ebert, M. Boutros, The drug-induced phenotypic landscape of colorectal cancer organoids, Nat. Commun. 13 (1) (2022).
[174] B.M. Larsen, M. Kannan, L.F. Langer, B.D. Leibowitz, A. Bentaieb, A. Cancino, et al., A pan-cancer organoid platform for precision medicine, Cell Rep. 36 (4) (2021).
[175] J. Culley, P.W. Nagle, J.C. Dawson, N.O. Carragher, Patient derived glioma stem cell spheroid reporter assays for live cell high content analysis, SLAS Discov Adv Life Sci R D. 28 (2) (2023) 13–19.
[176] S.N. Varadarajan, K.A. Mathew, A. Chandrasekharan, S.S. Lupitha, A. Lekshmi, M. Mini, P. Darvin, T.R. Santhoshkumar, Real-time visualization and quantitation of cell death and cell cycle progression in 2D and 3D cultures utilizing genetically encoded probes, J. Cell. Biochem. 123 (4) (2022) 782–797.
[177] C. Vianello, F. Dal Bello, S.H. Shin, S. Schiavon, C. Bean, A.P. Magalhães Rebelo, et al., High-Throughput Microscopy Analysis of Mitochondrial Membrane Potential in 2D and 3D Models, Cells. 12 (7) (2023) 1089.
[178] C. Wenzel, B. Riefke, S. Gründemann, A. Krebs, S. Christian, F. Prinz, M. Osterland, S. Golfier, S. Räse, N. Ansari, M. Esner, M. Bickle, F. Pampaloni, C. Mattheyer, E.H. Stelzer, K. Parczyk, S. Prechtl, P. Steigemann, 3D high-content screening for the identification of compounds that target cells in dormant tumor spheroid regions, Exp. Cell Res. 323 (1) (2014) 131–143.
[179] S.J. Kochanek, D.A. Close, P.A. Johnston, High Content Screening Characterization of Head and Neck Squamous Cell Carcinoma Multicellular Tumor Spheroid Cultures Generated in 384-Well Ultra-Low Attachment Plates to Screen for Better Cancer Drug Leads, Assay Drug Dev. Technol. 17 (1) (2019) 17–36.
[180] S.J. Kochanek, D.A. Close, D.P. Camarco, P.A. Johnston, Maximizing the Value of Cancer Drug Screening in Multicellular Tumor Spheroid Cultures: A Case Study in Five Head and Neck Squamous Cell Carcinoma Cell Lines, SLAS Discov Adv Life Sci R D. 25 (4) (2020) 329–349.
[181] T.H. Booij, W.N. Leonhard, H. Bange, K. Yan, M. Fokkelman, A.J. Plugge, et al., In vitro 3D phenotypic drug screen identifies celastrol as an effective in vivo inhibitor of polycystic kidney disease, J Mol Cell Biol. 12 (8) (2020) 644–653.
[182] B.J. Engel, P.E. Constantinou, L.K. Sablatura, N.J. Doty, D.D. Carson, M.C. Farach-Carson, D.A. Harrington, T.I. Zarembinski, Multilayered, Hyaluronic Acid-Based Hydrogel Formulations Suitable for Automated 3D High Throughput Drug Screening of Cancer-Stromal Cell Cocultures, Adv. Healthc. Mater. 4 (11) (2015) 1664–1674.
[183] I. Nassiri, M.N. McCall, Systematic exploration of cell morphological phenotypes associated with a transcriptomic query, Nucleic Acids Res. 46 (19) (2018).
[184] N. Moshkov, T. Becker, K. Yang, P. Horvath, V. Dancik, B.K. Wagner, P. A. Clemons, S. Singh, A.E. Carpenter, J.C. Caicedo, Predicting compound activity from phenotypic profiles and chemical structures, Nat. Commun. 14 (1) (2023).
[185] W. Wang, D. Douglas, J. Zhang, S. Kumari, M.S. Enuameh, Y. Dai, C.T. Wallace, S. C. Watkins, W. Shu, J. Xing, Live-cell imaging and analysis reveal cell phenotypic transition dynamics inherently missing in snapshot data, Sci. Adv. 6 (36) (2020).
[186] C.E. Mills, K. Subramanian, M. Hafner, M. Niepel, L. Gerosa, M. Chung, C. Victor, B. Gaudio, C. Yapp, A.J. Nirmal, N. Clark, P.K. Sorger, Multiplexed and reproducible high content screening of live and fixed cells using Dye Drop, Nat. Commun. 13 (1) (2022).
[187] P.A. Sandoz, C. Tremblay, F.G. van der Goot, M. Frechin, S.L. Schmid, Image-based analysis of living mammalian cells using label-free 3D refractive index maps reveals new organelle dynamics and dry mass flux, PLoS Biol. 17 (12) (2019) e3000553.
[188] I. Buzalewicz, M. Mrozowska, A. Kmiecik, M. Kulus, K. Haczkiewicz-Leśniak, P. Dzięgiel, M. Podhorska-Okołów, Ł. Zadka, Quantitative Phase Imaging Detecting the Hypoxia-Induced Patterns in Healthy and Neoplastic Human Colonic Epithelial Cells, Cells. 11 (22) (2022) 3599.
[189] R. Kasprowicz, R. Suman, P. O'Toole, Characterising live cell behaviour: Traditional label-free and quantitative phase imaging approaches, Int. J. Biochem. Cell Biol. 84 (2017) 89–95.
[190] A. Puerta, A. González-Bakker, G. Santos, J.M. Padrón, Early Pharmacological Profiling of Antiproliferative Compounds by Live Cell Imaging, Mol Basel Switz. 27 (16) (2022) 5261.
[191] R.D. Abbott, D.L. Kaplan, Strategies for improving the physiological relevance of human engineered tissues, Trends Biotechnol. 33 (7) (2015) 401–407.
[192] I. Berger Fridman, J. Kostas, M. Gregus, S. Ray, M.R. Sullivan, A.R. Ivanov, S. Cohen, T. Konry, High-throughput microfluidic 3D biomimetic model enabling quantitative description of the human breast tumor microenvironment, Acta Biomater. 132 (2021) 473–488.
[193] L. Fang, Y. Liu, J. Qiu, W. Wan, Bioprinting and its Use in Tumor-On-A-Chip Technology for Cancer Drug Screening: A Review, Int J Bioprinting. 8 (4) (2022) 603.
[194] R. Shyam, L.V.K. Reddy, A. Palaniappan, Fabrication and Characterization Techniques of In Vitro 3D Tissue Models, Int J Mol Sci. 24 (3) (2023) 1912.
[195] P. Zarrintaj, M.R. Saeb, F.J. Stadler, M.K. Yazdi, M.N. Nezhad, S. Mohebbi, F. Seidi, M.R. Ganjali, M. Mozafari, Human Organs-on-Chips: A Review of the State-of-the-Art, Current Prospects, and Future Challenges, Adv Biol. 6 (1) (2022) e2000526.
[196] H. Wang, Y. Rivenson, Y. Jin, Z. Wei, R. Gao, H. Günaydın, L.A. Bentolila, C. Kural, A. Ozcan, Deep learning enables cross-modality super-resolution in fluorescence microscopy, Nat. Methods 16 (1) (2019) 103–110.
[197] Goldsborough P, Pawlowski N, Caicedo JC, Singh S, Carpenter AE. CytoGAN: Generative Modeling of Cell Images [Internet]. bioRxiv; 2017 [cited 2023 May 27]. p. 227645. Available from: https://www.biorxiv.org/content/10.1101/227645v1.
[198] P.A. Marin Zapata, O. Méndez-Lucio, T. Le, C.J. Beese, J. Wichard, D. Rouquié, D.-A. Clevert, Cell morphology-guided de novo hit design by conditioning GANs on phenotypic image features, Digit Discov. 2 (1) (2023) 91–102.
[199] M. Hofmarcher, E. Rumetshofer, D.A. Clevert, S. Hochreiter, G. Klambauer, Accurate Prediction of Biological Assays with High-Throughput Microscopy Images and Convolutional Networks, Journal of ChemistryInf Model. 59 (3) (2019) 1163–1171.